UNIVERSIDADE FEDERAL DO PARANÁ

ALINE GUIDOLIN DA LUZ

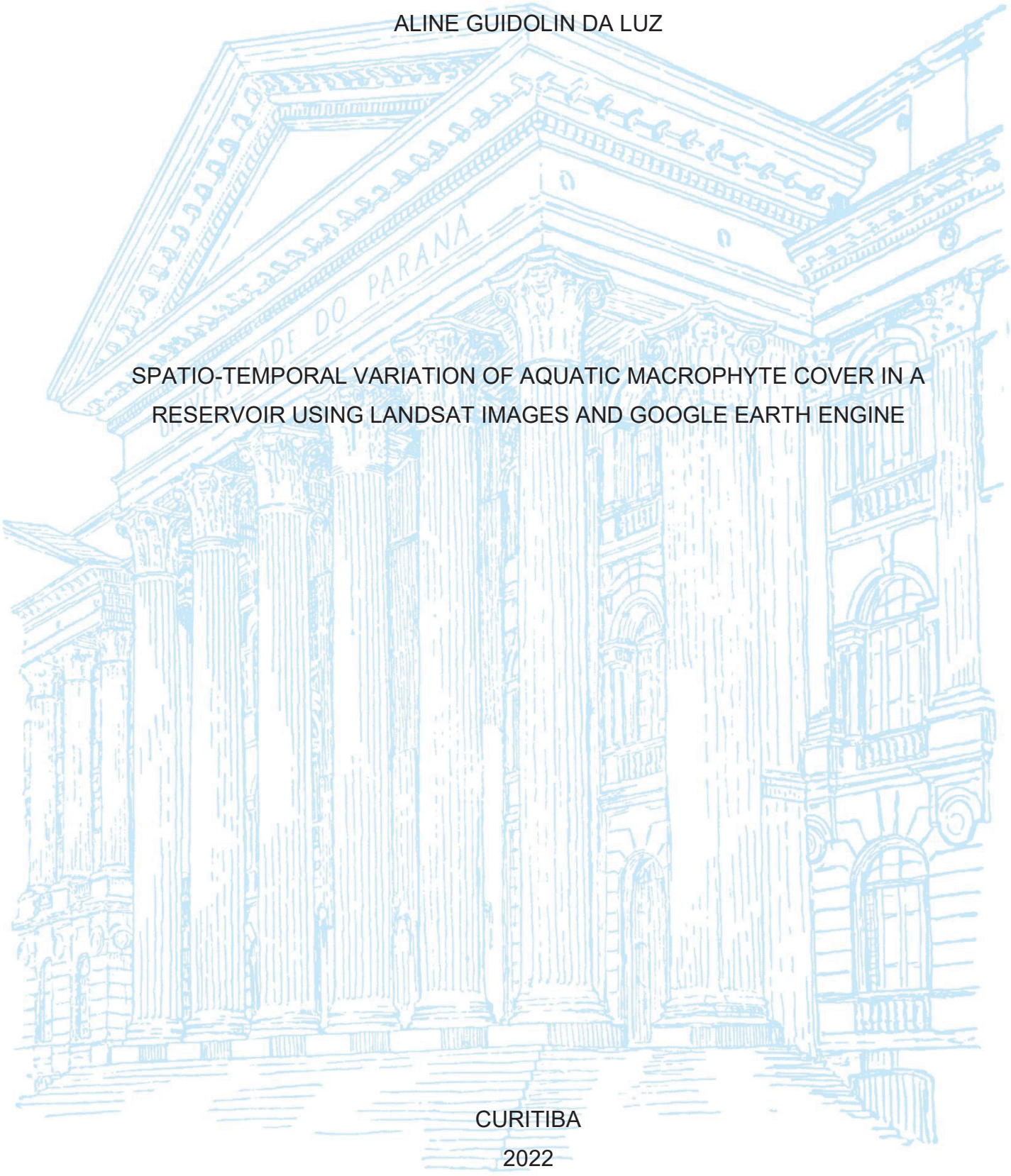

SPATIO-TEMPORAL VARIATION OF AQUATIC MACROPHYTE COVER IN A RESERVOIR USING LANDSAT IMAGES AND GOOGLE EARTH ENGINE

CURITIBA

2022

ALINE GUIDOLIN DA LUZ

SPATIO-TEMPORAL VARIATION OF AQUATIC MACROPHYTE COVER IN A RESERVOIR USING LANDSAT IMAGES AND GOOGLE EARTH ENGINE

Dissertação apresentada ao curso de Pós-Graduação em Engenharia de Recursos Hídricos e Ambiental, Setor de Tecnologia, Universidade Federal do Paraná, como requisito parcial à obtenção do título de Mestre em Engenharia de Recursos Hídricos e Ambiental.

Orientador: Prof. Dr. Tobias Bleninger.

Coorientadora: Dra.Bruna Arcie Polli.

CURITIBA

2022

DADOS INTERNACIONAIS DE CATALOGAÇÃO NA PUBLICAÇÃO (CIP)
UNIVERSIDADE FEDERAL DO PARANÁ
SISTEMA DE BIBLIOTECAS – BIBLIOTECA DE CIÊNCIA E TECNOLOGIA

Luz, Aline Guidolin da
Spatio-temporal variation of aquatic macrophyte cover in a reservoir using Landsat Images and Google Earth Engine / Aline Guidolin da Luz. – Curitiba, 2022.
1 recurso on-line : PDF.

Dissertação (Mestrado) - Universidade Federal do Paraná, Setor de Tecnologia, Programa de Pós-Graduação em Engenharia de Recursos Hídricos e Ambiental.

Orientador: Tobias Bernward Bleninger
Coorientador: Bruna Arcie Polli

1. Sensoriamento Remoto. 2. Plantas aquáticas. 3. Sazonalidade. 4. Vazante. 5. Macrófitas aquáticas. I. Universidade Federal do Paraná. II. Programa de Pós-Graduação em Engenharia de Recursos Hídricos e Ambiental. III. Bleninger, Tobias Bernward. IV. Polli, Bruna Arcie. V. Título.

Bibliotecário: Elias Barbosa da Silva CRB-9/1894

MINISTÉRIO DA EDUCAÇÃO
SETOR DE TECNOLOGIA
UNIVERSIDADE FEDERAL DO PARANÁ
PRÓ-REITORIA DE PESQUISA E PÓS-GRADUAÇÃO
PROGRAMA DE PÓS-GRADUAÇÃO ENGENHARIA DE RECURSOS HÍDRICOS E AMBIENTAL - 40001016021P0

TERMO DE APROVAÇÃO

Os membros da Banca Examinadora designada pelo Colegiado do Programa de Pós-Graduação ENGENHARIA DE RECURSOS HÍDRICOS E AMBIENTAL da Universidade Federal do Paraná foram convocados para realizar a arguição da dissertação de Mestrado de **ALINE GUIDOLIN DA LUZ** intitulada: **Spatio-temporal variation of aquatic macrophyte cover in a reservoir using Landsat images and Google Earth Engine**, sob orientação do Prof. Dr. TOBIAS BERNWARD BLENINGER, que após terem inquirido a aluna e realizada a avaliação do trabalho, são de parecer pela sua APROVAÇÃO no rito de defesa.

A outorga do título de mestra está sujeita à homologação pelo colegiado, ao atendimento de todas as indicações e correções solicitadas pela banca e ao pleno atendimento das demandas regimentais do Programa de Pós-Graduação.

CURITIBA, 12 de Agosto de 2022.

Assinatura Eletrônica
16/08/2022 17:55:26.0
TOBIAS BERNWARD BLENINGER
Presidente da Banca Examinadora

Assinatura Eletrônica
17/08/2022 07:38:08.0
GABRIEL HENRIQUE DE ALMEIDA PEREIRA
Avaliador Externo (SIMEPAR)

Assinatura Eletrônica
25/08/2022 14:56:46.0
JORGE ANTONIO SILVA CENTENO
Avaliador Interno (UNIVERSIDADE FEDERAL DO PARANÁ)

Assinatura Eletrônica
16/08/2022 17:42:18.0
HELOISE GARCIA KNAPIK
Avaliador Interno (UNIVERSIDADE FEDERAL DO PARANÁ)

AGRADECIMENTOS

Aos meus orientadores - Tobias Bleninger, Bruna Arcie Polli e Bernardo Lipski – obrigada por todo conhecimento compartilhado comigo nesses últimos dois anos. Através dele, hoje temos como fruto essa dissertação. Obrigada também por terem feito parte da formação da acadêmica e da profissional que sou hoje.

Ao professor Jorge Antonio Silva Centeno e à professora Heloise Garcia Knapik, agradeço por todas as orientações que contribuíram para esse trabalho.

Á UFPR e ao programa de Pós-Graduação em Engenharia de Recursos Hídricos e Ambiental (PPGERHA), especialmente a todas as professoras, professores e servidores, muito obrigada.

Ao Lactec e á CTG Brasil que, além de financiaram essa pesquisa, proporcionaram também uma bolsa de mestrado. Obrigada também aos colegas do Lactec, em especial ao João - pelo bom gosto musical em campo – e a Dani Drago.

À minha família. Meus pais Élliri e Francisco, e ao meu irmão Felipe, muito obrigada por todo o esforço em sempre proporcionar uma educação de qualidade, por contribuírem tanto para a formação do meu caráter e pelo apoio e amor incondicionais sempre.

Ao meu amor, Victor. Obrigada por caminhar ao meu lado ao longo desses anos, por cada palavra de incentivo, pela a paciência, pelo carinho de sempre e por fazer a vida ser mais leve.

Às minhas amigas Bruna, Francielle e Gabriela. Obrigada por todo companheirismo, de longe ou de perto. É muito bom crescer com vocês.

E a todos que de alguma maneira contribuíram para esta dissertação.

Muito obrigada!

RESUMO

A presença de grandes quantidades de macrófitas aquáticas em reservatórios pode desencadear diversos impactos no ecossistema local e o uso de metodologias convencionais para seu monitoramento, como coletas in loco, retorna apenas informações do momento presente. Com isso em vista, este estudo teve como objetivo mapear a variação espaço-temporal da cobertura de macrófitas utilizando imagens Landsat 5, 7 e 8 para o período de 1984-2021 no reservatório Jupiá. Também foram verificadas como algumas variáveis ambientais que impactam no crescimento de macrófitas (como variação do uso do solo, temperatura, precipitação e vazões de entrada no reservatório) se comportaram ao longo dos anos. Além disso, também foram construídas curvas e mapas da permanência de macrófitas nesse reservatório para serem usadas como base de comparação de novos mapeamentos. Para realizar isto, foi necessário determinar o melhor conjunto de índice espectral e intervalo de classificação das macrófitas. Como principais resultados, foram observadas variações interanuais na disposição espacial das macrófitas e tendência de crescimento da área, sendo este último possivelmente causado pela implantação de um reservatório a montante do reservatório Jupiá. Foi observado que além da magnitude da vazão, a forma como há incremento nas vazões também é relevante em termos de deslocamento de macrófitas dentro do reservatório. Apesar da quantidade de imagens sem interferências ter sido uma limitação, a construção de uma série histórica de ocupação de macrófitas se mostrou satisfatória e poderá auxiliar na tomada de decisões de manejo desses organismos.

Palavras-chave: Sensoriamento Remoto, Macrófitas aquáticas, Reservatório Jupiá, Tendência de crescimento, Sazonalidade, Vazões.

ABSTRACT

The presence of large amounts of aquatic macrophytes in reservoirs can trigger several impacts on the local ecosystem and the use of conventional methodologies for their monitoring, such as in loco activities, only returns information from the present moment. With that in mind, this study aimed to map the spatio-temporal variation of macrophyte cover using Landsat 5, 7 and 8 images for the period 1984-2021 at Jupiá reservoir, in southeast of Brazil. It was also verified how some environmental variables that impact the growth of macrophytes (such as variation in land use, temperature, precipitation and reservoir inflows) behaved over the years. In addition, curves and maps of the permanence of macrophytes in this reservoir were also constructed to be used as a basis for comparing new mappings. To accomplish this, it was necessary to determine the best set of spectral index and classification range of macrophytes. As main results, interannual variations were observed in the spatial arrangement of macrophytes and the area's growth trend, the latter possibly caused by the implementation of a reservoir upstream of the Jupiá reservoir. It was observed that in addition to the magnitude of the flow, the way in which there is an increase in the flows is also relevant in terms of the displacement of macrophytes within the reservoir. Although the number of images without interference was a limitation, the construction of a historical series of macrophyte occupation proved to be satisfactory and could help in decision-making for the management of these organisms.

Keywords: Remote sensing, Aquatic macrophytes, Jupiá Reservoir, Growth trend, Seasonality, Flows.

LIST OF FIGURES

FIGURE 1 - TYPES OF AQUATIC MACROPHYTES 16
FIGURE 2 - FACTORS THAT MAY CONTRIBUTE TO THE GROWTH AND DISPLACEMENT OF MACROPHYTES 17
FIGURE 3 - SOME TRANSFORMATIONS IN RIVERS RESULTING FROM THE FORMATION OF RESERVOIRS AND THEIR EFFECTS ON AQUATIC MACROPHYTES 18
FIGURE 4 – CONCEPTUAL DIAGRAM OF THE SUMA MODEL 19
FIGURE 5 - LOCATION, SOME OF THE MACROPHYTE SPECIES FOUND AND THE DEPTH OF THE JUPIÁ RESERVOIR 31
FIGURE 6 - AVERAGE MONTHLY INFLOWS[1] INTO THE JUPIÁ RESERVOIR BETWEEN 1984-2021; ANNUAL AND MONTHLY PRECIPITATION BETWEEN 1984-2021[2] AND AVERAGE MONTHLY TEMPERATURE[3] AT ILHA SOLTEIRA STATION BETWEEN 1991-2021 32
FIGURE 7 - AQUATIC MACROPHYTES CLASSIFICATION PROCESS FLOWCHART IN LANDSAT 5, 7 AND 8 IMAGES. 33
FIGURE 8 - FIELD RESEARCH PHOTOGRAPHIC RECORDS AND DETAILS OF WATER, AQUATIC MACROPHYTES AND OTHER VEGETATIONS SAMPLE POINTS 35
FIGURE 9 - VEGETATION AND PERMANENT SETTLEMENT DETAILING AT FERRADURA ISLAND, ON PARANÁ RIVER. 35
FIGURE 10 - EXAMPLE OF ERRORS PRESENT IN IMAGES WHICH WERE DISCARDED AFTER VISUAL ANALYSIS 36
FIGURE 11 - FREQUENCY DIAGRAMS OF RED, GREEN AND NIR BANDS, AND NDVI, GNDVI AND GSAVI SPECTRAL INDICES CONSIDERING 70% OF THE WATER, MACROPHYTE AND OTHER VEGETATION DATA. 39
FIGURE 12 - FIT OF MACROPHYTE AND OTHERS VEGETATION DATA TO NORMAL DISTRIBUTIONS. 40
FIGURE 13 - AQUATIC MACROPHYTES IDENTIFICATION IN THE LANDSAT 8 IMAGE FOR 03/05/2017. 41
FIGURE 14 - AQUATIC MACROPHYTES IDENTIFICATION IN THE LANDSAT 8 IMAGE FOR 06/07/2017. 42

FIGURE 15 - MACROPHYTE COVERAGE AREA HISTORICAL SERIES FOR THE 142 IMAGES SELECTED USING GSAVI INDEX (0.024 - 0.294) AND PRESENTED BY SEASON.....44
FIGURE 16 - MAXIMUM AND MINIMUM AREAS OF MACROPHYTES AND LINEAR TREND CURVE FIT.....44
FIGURE 17 - MACROPHYTE COVERAGE AREA PERMANENCE CURVES FOR EACH DECADE (1984-1989, 1990-1999, 2000-2009 AND 2010-2021), FOR THE ENTIRE HISTORICAL SERIES (1984-2021) AND ITS RESPECTIVE POLYNOMIAL ADJUSTMENT CURVE 45
FIGURE 18 - BOXPLOT OF THE MACROPHYTE AREAS VARIATION EACH DECADE 46
FIGURE 19 - MACROPHYTE COVERAGE AREA PERMANENCE CURVES FOR EACH SEASON (SUMMER, AUTUMN, WINTER AND SPRING), FOR THE ENTIRE HISTORICAL SERIES (1984-2021) AND ITS RESPECTIVE POLYNOMIAL ADJUSTMENT CURVE.....47
FIGURE 20 - BOXPLOT OF THE MACROPHYTE AREAS VARIATION IN EACH SEASON OF THE YEAR. 47
FIGURE 21 - PERMANENCE CURVE OF MAXIMUM MACROPHYTE AREAS AND ITS RESPECTIVE LINEAR ADJUSTMENT. 48
FIGURE 22 - RETURN TIME CURVE OF MAXIMUM MACROPHYTE AREAS AND ITS RESPECTIVE LOGARITHMIC FIT.....48
FIGURE 23 - MACROPHYTE PERMANENCE MAP FOR THE ENTIRE PERIOD 1984-2021* (*EXCEPT FOR THE YEARS: 2003, 2011, 2012 AND 2013). 50
FIGURE 24 - PERMANENCE MAP DETAILING FOR THE TIETÊ RIVER REGION WITH VARIATIONS BETWEEN SEASONS AND DECADES.....51
FIGURE 25 - PERMANENCE MAP DETAILING FOR THE PARANÁ RIVER REGION WITH VARIATIONS BETWEEN SEASONS AND DECADES.....52
FIGURE 26 - PERMANENCE MAP DETAILING FOR THE SUCURIÚ RIVER REGION WITH VARIATIONS BETWEEN SEASONS AND DECADES. 53

FIGURE 27 - LAND USES VARIATION IN THE JUPIÁ WATERSHED AND IN THE INCREMENTAL WATERSHEDS (ILHA SOLTEIRA, TRÊS IRMÃOS AND SUCURIÚ) BETWEEN 1985 AND 2020. 54
FIGURE 28 - SEASONAL VARIATION OF MONTHLY PRECIPITATION, MONTHLY MEAN TEMPERATURE AND MACROPHYTE AREA OVER 2014-2021. 55
FIGURE 29 - MAXIMUM MONTHLY (HOURLY) OUTFLOW, SPILLWAY AND TURBINE DISCHARGE AT ILHA SOLTEIRA AND TRÊS IRMÃOS HPP.....56
FIGURE 30 - COMPARISON BETWEEN JUNE/2016 AND MAY/2017 OPERATIONS IN TRÊS IRMÃOS HPP. 57

LIST OF TABLES

TABLE 1 - SUMMARIES OF STUDIES THAT VERIFY LIMITING FACTORS FOR AQUATIC MACROPHYTE GROWTH.....24
TABLE 2 - SUMMARIES OF STUDIES THAT PERFORMED MODELING AND HYDROACUSTIC SURVEYS OF AQUATIC MACROPHYTES.....25
TABLE 3 - SUMMARIES OF SEVERAL APPLICABILITY STUDIES THAT MADE REMOTE SENSING USE 26
TABLE 4 - SUMMARIES OF STUDIES LINKED TO WATER QUALITY PARAMETERS USING REMOTE SENSING.....27
TABLE 5 - SUMMARIES OF STUDIES LINKED TO MONITORING MACROPHYTES USING REMOTE SENSING 28
TABLE 6 - SUMMARIES OF STUDIES LINKED TO REMOTE SENSING USING THE GOOGLE EARTH ENGINE (GEE).....29
TABLE 7 - COHEN'S KAPPA COEFFICIENT REFERENCES.....36
TABLE 8 - AQUATIC MACROPHYTE CLASSIFICATION CONFUSION MATRICES AND MODEL ACCURACY.....41
TABLE 9 - QUANTITY AND TEMPORAL IMAGES DISTRIBUTION USED TO COMPOSE THE MACROPHYTE COVERAGE TIME SERIES BETWEEN 1984-2021. 43

CONTENTS

1 INTRODUCTION 12
1.1 HYPOTHESIS 13
1.2 OBJECTIVES 13
2 LITERATURE REVIEW 14
2.1 SENSORIAMENTO REMOTO 14
2.2 AQUATIC MACROPHYTES 16
2.3 MONITORING OF MACROPHYTES 17
3 MATERIAL AND METHODS 30
3.1 STUDY AREA DESCRIPTION 30
3.2 MACROPHYTES IDENTIFICATION IN LANDSAT IMAGES 33
3.3 CURVES AND MAPS OF MACROPHYTE AREA PERMANENCE 37
3.4 ENVIRONMENTAL VARIABLES EFFECTS ON MACROPHYTE GROWTH 37
4 RESULTS AND DISCUSSIONS 38
4.1 MACROPHYTES IDENTIFICATION IN LANDSAT IMAGES 38
4.2 MACROPHYTE AREA HISTORICAL SERIES 42
4.3 MACROPHYTE AREA PERMANENCE CURVE 44
4.4 MACROPHYTE AREA PERMANENCE MAPS 49
4.5 ENVIRONMENTAL VARIABLES EFFECTS ON MACROPHYTE GROWTH 53
4.5.1 Land use analysis 53
4.5.2 Temperature and precipitation analysis 54
4.5.3 Upstream HPP discharge analysis 55
5 FINAL CONSIDERATIONS 58
ACKNOWLEDGEMENTS 59
REFERENCES 59

1 INTRODUCTION

Brazil has more than 1300 power generation construction from hydraulic sources (ANEEL, 2019), in order to the energy matrix is composed of more than 65% of sources of this nature (BRASIL, 2021).

Infrastructure for hydraulic energy generation, such as the damming of rivers to form reservoirs, causes changes in region's ecosystem and in the river's hydrodynamics. The increased propensity to accumulate nutrients in the reservoir region is an imbalance that, combined with the characteristics of tropical and subtropical climates, such as high temperatures and high solar incidence, can trigger the proliferation of aquatic macrophytes. This happened at the Engenheiro Souza Dias Hydropower Plant - HPP (located on the border between the states of São Paulo and Mato Grosso do Sul, Brazil), witch in large quantities of aquatic macrophytes were responsible for interruptions in energy generation through the obstruction of the water intake conduits in May/2017, making a total of 10 generating units unavailable for about 5 months and causing losses about R$ 3.8 million in maintenance only (CTG Brasil, 2019). These organisms must be monitored as a result of negatively impact to the environment, reducing the diversity of floristic species, causing fauna's mortality, besides damage and interruptions in energy generation (ESTEVES, 1998).

Conventional monitoring methodologies used to quantify aquatic macrophytes can be costly and time-consuming (LUO et al., 2016; ZHAO et al., 2012), given the extensive area of the reservoirs. Moreover, the sample universe obtained by conventional methodologies only includes present information. So, the use of remote sensing as a complementary tool to on-site monitoring has proved to be an interesting alternative to reduce this problem, both due to the amount and availability of data, as well as the possibility of recall old information and, which enables observing the historical evolution of macrophyte growth in reservoirs (BAI et al., 2020; COLADELLO et al., 2020; LUO et al., 2016). In addition, even using images taken from short periods, it is possible to verify the presence or absence of specific behaviors between different periods of the year (MINHONI et al., 2017; TENA et al., 2017) or even verify the influence of anthropic activities or climate change in the growth of macrophytes (BEZERRA JUNIOR, 2021; LIMA et al., 2018; MINHONI et al., 2018).

1.1 HYPOTHESIS

It is considered that knowing the spatial and temporal evolution of macrophytes in reservoirs is relevant in decision-making regarding reservoirs operation and in the management actions of these organisms.

1.2 OBJECTIVES

In this context, the aim of the present study was to verify if there was trend growth of aquatic macrophytes through the determination of the historical series of the macrophytes area by remote sensing and the spatio-temporal variation of aquatic macrophytes in the Jupiá reservoir (Engenheiro Souza Dias HPP), between 1984-2021. It was also analyzed if climatic characteristics of the region (precipitation and temperature) reproduced any interannual seasonal behavior in the macrophytes cover, and if the land use change and the operations of upstream hydropower plants contributed to the increase in the area of macrophytes over the years.

Besides, permanence curves of the macrophyte area will also be constructed to serve as a tool for comparison with new monitored areas. In the same way, permanence maps will be do for the spatial distribution comparison of new mappings.

For this, some intermediate points need to be met:

a) Determine the best set of spectral index and respective range to identify macrophytes in the images.
b) Analyze whether there are interannual patterns - like seasonality - in the spatial and temporal coverage of macrophytes.
c) Check how some environmental variables impacted the growth of macrophytes over the years.

2 LITERATURE REVIEW

In this chapter of literature review, initially and briefly, the description of basic concepts relevant to the topic addressed in this work will be presented, such as definitions of remote sensing and aquatic macrophytes. A review of previously developed studies that address the environmental monitoring of aquatic macrophytes and other studies that use remote sensing as a monitoring tool will also be presented. Finally, some benefits and uses of the Google Earth Engine tool in the processing of satellite images will be discussed.

2.1 SENSORIAMENTO REMOTO

The term remote sensing refers to *“uma ciência que visa o desenvolvimento da obtenção de imagens da superfície terrestre por meio da detecção e medição quantitativa das respostas das interações da radiação eletromagnética com os materiais terrestres”* (MENESES; ALMEIDA, 2012, p. 3).

These images have spatial resolution, which is equivalent to the size of the smallest object that can be identified in an image. Images with large spatial resolution provide high detail of objects, while small resolutions generate less detail (MENESES; ALMEIDA, 2012). In other words, images with a resolution of 30 meters, such as Landsat images, are not able to identify objects with dimensions smaller than 30 x 30 meters, but Sentinel-2 images would, because their resolution is 10 meters. Also, the temporal resolution is linked to the interval between two images, that is, the time interval in which two images are recorded in the same area.

The different types of matter existing on the Earth's surface have different reflectances, that is, they stand out at different wavelengths, and it is this characteristic that allows their distinction. In this context, the spectral resolution of an image is the property that relates the amount of subdivisions of wavelengths into spectral bands and the size of the length of each band (MENESES; ALMEIDA, 2012) .

The result of some algebraic operations with the spectral bands can give rise to a spectral index, which relate one or more bands in order to highlight a particular object, such as water or vegetation. Of the spectral indices most commonly used to identify vegetation, one can cite the NDVI - Normalized Difference Vegetation Index - which uses the red and near-infrared bands due to chlorophyll activity, because the

healthier the vegetation, the more it absorbs light in the red region and reflects in the near-infrared region. As the index can vary between -1 and 1, results close to 1 indicate areas with healthy vegetation, negative values represent areas such as water and clouds, while null values indicate absence of vegetation (CORDEIRO et al., 2017; ROUSE et al., 1973).

$$NDVI = \frac{(R_{NIR} - R_{Red})}{(R_{NIR} + R_{Red})}$$

in which R is the reflectance and NIR and Red are the near infrared and red bands, respectively.

In the same logic is the GNDVI index - Green Normalized Difference Vegetation Index - which also results in values between -1 and 1 and has the same classifications as the NDVI, but is more sensitive to the variation of chlorophyll activity (GITELSON; KAUFMAN; MERZLYAK, 1996). It is recommended to use this index for well-developed vegetation, while the NDVI for younger vegetation.

$$GNDVI = \frac{(R_{NIR} - R_{Green})}{(R_{NIR} + R_{Green})}$$

in which R is the reflectance and NIR and Green are the near infrared and green bands, respectively.

The SAVI index – Soil-Adjusted Vegetation Index - was developed based on the NDVI, but considering a correction factor for soil effects (L) such as color, moisture and spatial variability (HUETE, 1988). This factor varies between 0 and 1 depending on the density of the vegetation cover (1 for denser vegetation and 0 for less dense), but has been used as 0.5 in most cases (LIMA et al., 2017). Like GNDVI, GSAVI is a modification of the original index using the green band instead of the red band:

$$GSAVI = 1{,}5 \cdot \left(\frac{(R_{NIR} - R_{Green})}{(R_{NIR} + R_{Green} + 0{,}5)}\right)$$

in which R is the reflectance and NIR and RED are the near infrared and green bands, respectively.

2.2 AQUATIC MACROPHYTES

Aquatic macrophytes are highly adaptive organisms that, throughout the evolution process, migrated from water to the terrestrial environment, and then returned to water. For this reason, they are found in places with different characteristics such as brackish and salty environments, in hot springs, in rivers and lakes, among others, and are classified into ecological groups, according to the degree of adaptation to water: emerged, with floating leaves, submerged rooted, submerged free and floating (FIGURE 1) (TUNDISI; TUNDISI, 2008).

FIGURE 1 - TYPES OF AQUATIC MACROPHYTES

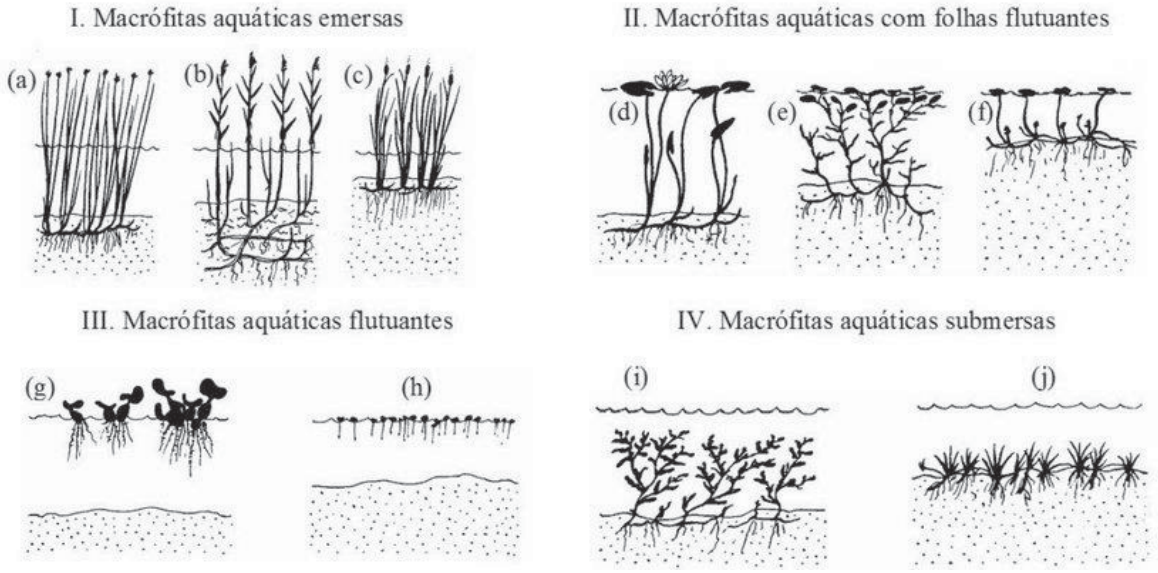

SOURCE: BRIX; CHIERUP (1989).

Within the reservoirs, the coastal region, which comprises the banks, is the region with the highest propensity to find macrophytes, since this area has greater interaction between water and land. In addition, macrophytes play an important role for other organisms by providing a reduction in water turbulence, by contributing to the cycling of nutrients through the pumping effect, by having high rates of primary productivity and by serving as food and refuge for other organisms (ESTEVES, 1998).

The aquatic macrophytes life cycle is slightly short and their growth is limited by factors such as temperature, nutrient availability, light availability and the action of herbivores (TUNDISI; TUNDISI, 2008). Besides, there are factors that provide the

permanence and development of these organisms, such as ponds or more sheltered areas, and others that cause their displacement, such as wind or current speed (FIGURE 2). In scenarios with intense macrophyte occupation, when these are in the process of decomposition, there is an increase in the amount of available organic matter, contributing to the growth of new individuals (BIANCHINI JUNIOR, 2003).

FIGURE 2 - FACTORS THAT MAY CONTRIBUTE TO THE GROWTH AND DISPLACEMENT OF MACROPHYTES

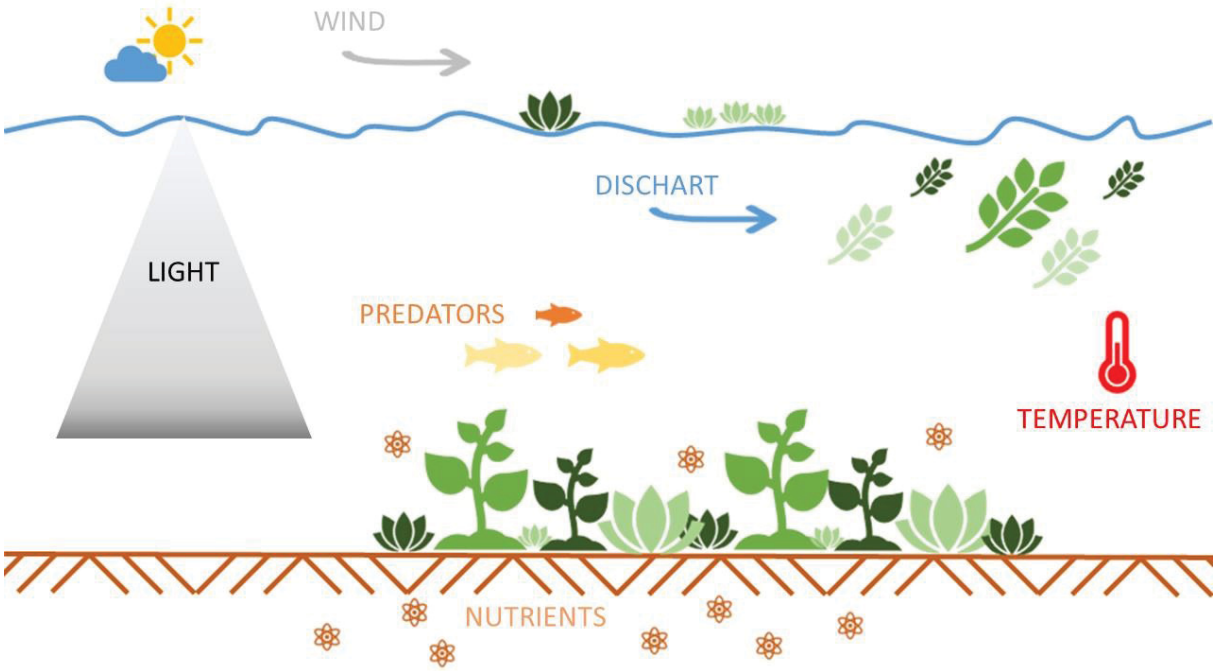

SOURCE: The Author (2022).

2.3 MONITORING OF MACROPHYTES

The monitoring of aquatic macrophytes is one of the tools that serves as a basis for various decision-making in the management of the water uses, such as actions to manage these organisms (POMPÊO, 2017). The use of aquatic macrophytes as bioindicators of water quality is one of the most relevant reasons for monitoring, either because of the presence or absence of these organisms, or because of their dynamics in the environment (CAMARGO; PEZZATO; HENRY-SILVA, 2003).

A portion of the studies that involve the monitoring of aquatic macrophytes verify the factors that influence the growth of the plants, in laboratory scale. Samples of these vegetables are grown in controlled conditions, using different concentrations

of nutrients (BIUDES; CAMARGO, 2008; FREITAS; SIDINEI, 2011; GIMENES et al., 2020), temperature, due to the speed of chemical reactions in organisms (MACHADO, 2020) and time of sun exposure, the main source of energy for photosynthetic processes (CANCIAN; CAMARGO; SILVA, 2009). In general, it was noted that anthropic activities and artificial eutrophication provide greater growth of different types of aquatic macrophytes. The damming of rivers was a highlight, which through changes in level and speed, in addition to accumulating nutrients, impact the production of these organisms (FIGURE 3). Furthermore, these studies highlight two points: the lack of studies on what impacts the activities of these vegetables in Brazil; and that existing studies focus on abundant organisms in their respective study regions.

FIGURE 3 - SOME TRANSFORMATIONS IN RIVERS RESULTING FROM THE FORMATION OF RESERVOIRS AND THEIR EFFECTS ON AQUATIC MACROPHYTES

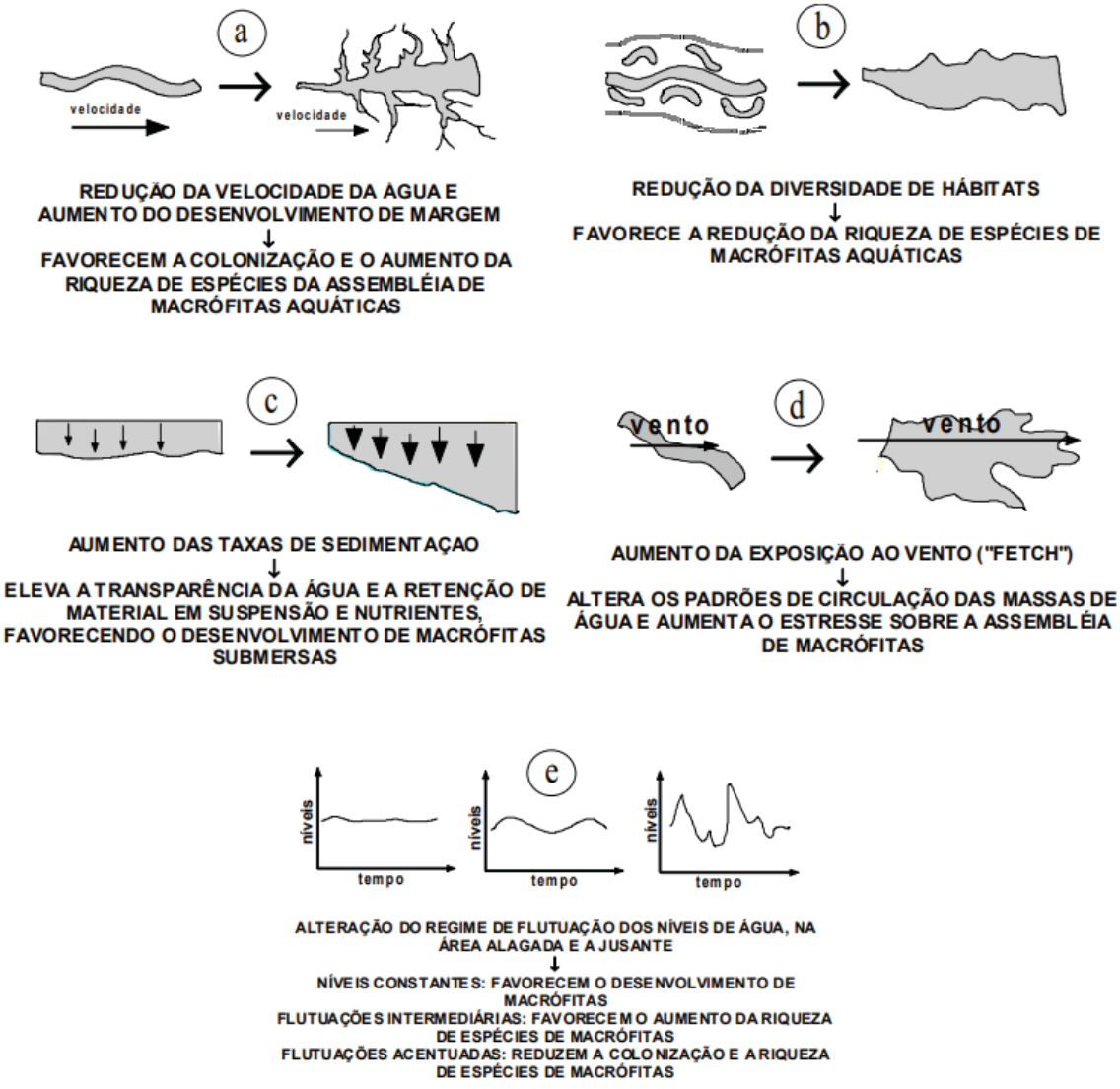

SOURCE: THOMAZ (2002).

Another group of studies sought to carry out the mathematical modeling of aspects of aquatic macrophytes, such as growth estimation (LACTEC, 2019b), interaction with other organisms such as phytoplankton and epiphyton (ASAEDA et al., 2000; ZHANG et al., 2015) decomposition of vegetables (CUNHA-SANTINO; BIANCHINI JR, 2006) according to single and double exponential models, and mainly of nutrients (GIUSTI; MARSILI-LIBELLI, 2005; SILVA , 2015; ZHANG et al., 2016). In these cases, a relevant differential of the modeling is the possibility of estimating the consequences in different scenarios, either with actions or in the absence of them, serving as a basis for interventions.

The SuMa model (Submerged Macrophyte), developed by LACTEC (2019a), is a mathematical model of macrophyte dynamics aimed at predicting biomass. For that, factors favorable to growth such as luminosity (Secchi disk), nutrients (phosphorus and nitrogen), temperature and depth of the site, and unfavorable factors implemented such as losses by waves and wind (FIGURE 4) are considered. The model was spatially evaluated by comparing its results and estimates of macrophyte coverage by satellite images, and so far, has had satisfactory results for the presence and absence of macrophytes in 93% of cases. However, the modeling results were overestimating the macrophyte area compared to the satellite image result, and the authors assume that this is due to the 200m resolution of the adopted grid.

FIGURE 4 – CONCEPTUAL DIAGRAM OF THE SUMA MODEL

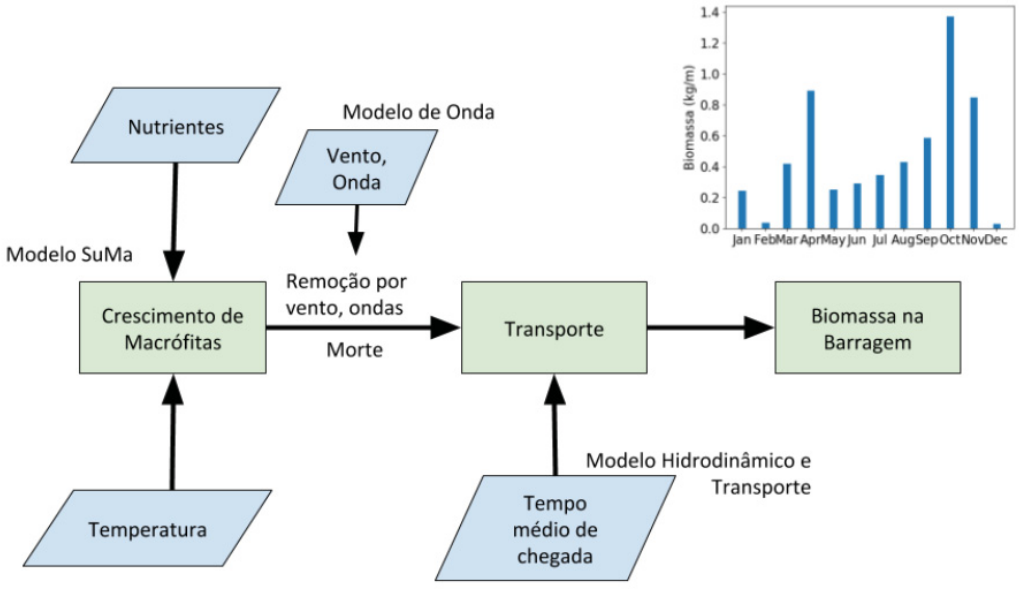

SOURCE: LACTEC (2019a).

ASAEDA et al. (2000) performed the modeling of a hypothetical lake to assess how the external load of nutrients, water temperature, depth and water retention time would imply the growth of macrophytes and phytoplankton, given predetermined biological characteristics. It was observed that, slowly, the amount of macrophytes decreases as there is an increase in the entry of nutrients and an increase in the amount of light penetration due to the phytoplankton biomass. In the same way, higher temperatures have a harmful effect on phytoplankton flowering, reducing their shadows, and promoting the consequent growth of macrophytes.

The modeling carried out in the study by SILVA (2015) uses a predator-prey system that encompasses the population dynamics of two species of macrophytes (prey) that are in competition for an available pollutant load, and the population dynamics of fish (predators). The solution of the equations on the spatial scale is given by the linear triangular Finite Element Method, while on the time scale it is by the Crank-Nicolson Method. The author corroborated the use of macrophytes as an indicator of water quality, since in his results, there was an increase in the biomass of these organisms in the places affected by the pollutant, in addition to punctuating the presence of wind as a limiting factor to the growth of macrophytes.

In the last decades, the use of satellite images as a tool has been widely used for several purposes, among which the assessment of possible consequences of climate change, monitoring of vegetation cover in forests, mapping of land use, and numerous applications in agriculture (PAN et al., 2018; WANG et al., 2018; WU et al., 2019).

GALO et al. (2002) used ETM+ Landsat orbital images to verify the occurrence of aquatic macrophytes in reservoirs of hydroelectric power plants of the Tietê complex, in São Paulo, Brazil, and determined strategic points of in loco monitoring. The results were obtained by the *Spring software* and pointed to the use of satellite images in the monitoring and management of large reservoirs as something very useful and to supplement field activities.

Also making use of Landsat images and *Spring* software, MESQUITA et al. (2013) monitored the occupation of macrophytes in the Umarí dam (Rio Grande do Norte, Brazil), in different periods of drought and rain. For the detection of macrophytes, the near infrared, red and green bands were used. Results obtained showed that the spatial distribution of rainfall was one of the limiting factors for

vegetation growth, and periods of low rainfall were considered favorable for development.

Likewise, ROSA et al. (2017) verified whether hydrological conditions of drought and rain influenced the dynamics of aquatic macrophytes in Banhado do Taim (Rio Grande do Sul, Brazil), also using Landsat satellite images and over a period of approximately 20 years. The analyzes were carried out in ArcGIS software and hydrological conditions considered within the normal range were related to a good biodiversity in the region, while in periods of drought there was an increase in the area of occurrence of some species.

The work developed by LIMA; LIBORIO; HADAD (2018) verified the presence of macrophytes in the Paraíba do Sul River through high resolution images (GeoEye-1 sensor) and related the results with water quality monitoring data obtained by the local utility. According to the authors, the increase in population in the cities of the region may have contributed to the increase in the coverage of aquatic macrophytes, since there was an increase in the concentration of nutrients in the water as a result of human activities.

COLADELLO et al. (2020) verified the temporal and spatial evolution of the coverage of aquatic macrophytes in the reservoir of the Salto Grande hydroelectric plant in Campinas (São Paulo, Brazil), an area with high industrial and urban activity. For the detection of macrophytes, images from Landsat 5, 7 and 8 satellites were used and the NDVI was calculated, from 1984 to 2017, on a quarterly scale. With these data, analyzes were later carried out to verify trends, in addition to the occurrence and persistence of plants in certain regions. As one of the results, the areas with the presence of plants considered as critical were mapped.

Another important study that also has the Jupiá reservoir as its object of study was the previously mentioned P&D 10381-0317, which applied remote sensing techniques to monitor the growth and displacement of aquatic macrophyte banks and has as main result the implementation of a Macrophyte Monitoring System (SMM). Therefore, hydrodynamic and hydrological modeling were carried out, as well as limnological, floristic and bathymetric surveys, in addition to the detection of macrophytes from Sentinel-2 multispectral images and biotic parameters, such as Secchi disk, absorption coefficient, turbidity and total solids suspensions. However, despite the high spatial resolution that Sentinel-2 images present, the operation of this satellite only started in 2017, which makes analysis prior to that date impossible.

Another point of this project that deserves to be highlighted is the elaboration of an alert system that gathers meteorological data, flow from plants, water quality parameters and area occupied by macrophytes, to calculate the criticality of the growth and detachment of the banks. of macrophytes in the reservoir. This system gathers the variables that most significantly interfere in the alert calculation in a very intuitive interface, which makes it possible to take emergency operational actions (CTG Brasil, 2021).

On the other hand, the use of the Google Earth Engine (GEE) platform has been shown to be an indispensable instrument, given the possibilities provided by the rapid cloud processing of large amounts of data, making the use of supercomputers unnecessary (MUTANGA; KUMAR, 2019; TAMIMINIA et al., 2020) .

LOBO et al. (2021), cited above, developed a free platform on the GEE (Algae Bloom Monitoring Application – AlgaeMAp) that provides water quality parameters, such as information on algal blooms, chlorophyll and turbidity. The Sentinel-2 satellite, with data from August 2015 onwards, is used to calculate the Normalized Difference Chlorophyll-a Index (NDCI), which serves as the basis for calculating chlorophyll and Trophic State Index. This application includes the main reservoirs in the state of São Paulo and is expanding its database to encompass the main reservoirs in Latin America.

The work by LI et al. (2021) has Lake Chad as a study area , located in the Sahara desert and used for supply in Nigeria, Niger, Cameroon and Chad. The GHG was used to obtain the water cover series, in addition to flood areas that include, among other aspects, waters under macrophytes. The period analyzed was between the years 1980 and 2020, with NDVI images from several satellites.

In the same way, other authors used the GHG together with artificial intelligence methods to obtain the surface water extension, such as WANG et al. (2018) who processed 2,343 Landsat images from the 1990s, 2000s and 2010s, which underwent treatments to minimize cloud interference, in the Yangtze River basin (680,000 km²), in China.

Therefore, to condense the studies analyzed in this literature review, the main points to be highlighted in each study will be summarized below. The studies were grouped into categories: limiting factors for the growth of aquatic macrophytes (TABLE 1), modeling and hydroacoustic surveys of aquatic macrophytes (TABLE 2), various applications that made use of remote sensing (TABLE 3), water quality parameters

with use of remote sensing (TABLE 4), monitoring of macrophytes using remote sensing (TABLE 5) and remote sensing using Google Earth Engine (GEE) (TABLE 6).

It is noteworthy that the differential of this dissertation for the studies presented is to associate several points presented (such as limiting factors, remote sensing and analysis of long periods of time, facilitated by the GEE platform) in a single analysis.

TABLE 1 - SUMMARIES OF STUDIES THAT VERIFY LIMITING FACTORS FOR AQUATIC MACROPHYTE GROWTH

	STUDY	OBJECTIVE	STUDY AREA	EVALUATED PARAMETERS	MAIN RESULT
Limiting factors	DE FREITAS; SIDINEI, 2011	Assess whether the growth of Egeria najas and E. densa is limited by inorganic carbon	UHE Rosana Reservoir	inorganic carbon	Greater development of submerged species occurred in places with higher alkalinity values.
	GIMENES et al., 2020	To evaluate the toxicity c	Residues from the Fundão dam failure	Temperature, aluminum and manganese	Al and Mn caused harmful effects on the analyzed species and to a greater extent at higher temperatures (27 °C)
	MACHADO, 2020	Evaluate the growth of Egeria densa under different temperatures and turbidity	-	Temperature, turbidity and nutrient content in the soil	Temperature positively influenced growth For soils with composition: **Nitrogen:** tended to slow growth. **Potassium:** contributed to increased growth; **Phosphor:** statistically not significant; **Turbidity:** may not have caused significant interference with growth.
	CANCIAN; CAMARGO; SILVA, 2009	To evaluate the influence of temperature and photoperiod on the growth of Pistia stratiotes	Aguapeú River (Itanhaém River Basin)	temperature and photoperiod	The species is sensitive to low temperatures and high temperatures are also unfavorable; The species was not affected by photoperiod at normal temperatures, but at low temperatures growth is greater with longer photoperiod.

SOURCE: The Author (2022).

TABLE 2 - SUMMARIES OF STUDIES THAT PERFORMED MODELING AND HYDROACUSTIC SURVEYS OF AQUATIC MACROPHYTES

	STUDY	OBJECTIVE	STUDY AREA	EVALUATED PARAMETERS	MODEL	MAIN RESULT
Modeling and surveys	GIUSTI; MARSILI-LIBELLI, 2005	Carry out modeling to predict the development of macrophytes on and macroalgae and test actions to favor macrophytes	Orbetello Lagoon, Italy	Nutrients and submerged vegetation, dissolved oxygen, pH, conductivity, temperature, salinity and photoperiod	Hydrodynamic model + ecological model	The simulations reproduced recent observations in the lagoon and showed an evident net growth, which shows that in the current state the ecosystem is productive and confirms the need for vegetation control.
	SILVA, 2015	Evaluate the impact of macrophyte biomass on the presence of pollutants through the implementation of a predator-prey model	Salto Grande Reservoir, Sao Paulo, Brazil	Population of two macrophyte species (prey), a pollutant and fish population (predators).	Model of nonlinear partial differential equations, of the Diffusion-Advection-Reaction type	It corroborated that macrophytes are one of the main bioindicators of pollution, and there is an increase in biomass in the presence of pollutants and pointed out the wind as an important factor for limiting the production of macrophytes.
	ZHANG et al., 2016	Simulate the effect of macrophytes submerged in nutrients and by joining a water and macrophyte quality model	Yuqiao Reservoir, China	Total phosphorus, ammonia nitrogen, dissolved oxygen and chlorophyll-a	Yuqiao Reservoir Water Quality Model (YRWQM) and the macrophyte submodel	The integrated models present better results than the water quality model alone and a critical value of phosphorus was estimated for the transition from a clear to turbid water state.
	LACTEC, 2019a	Determine the biomass of macrophytes	Jupiá Reservoir, Sao Paulo, Brazil	Water depth, Secchi disk, radiation and initial biomass,	Differential equation model solved by the Runge-Kutta method	Biomass estimation over time
	SABO BOSCHI et al., 2012	Mapping aquatic macrophytes through hydroacoustic surveys	Porto Primavera Reservoir, Sao Paulo, Brazil	Water depth and plant height	echo sounder	Thematic map indicating variations in the volume of submerged aquatic plants
	LACTEC, 2019d	Mapping aquatic macrophytes through hydroacoustic surveys	Jupiá Reservoir, Sao Paulo, Brazil	Water depth and plant height	echo sounder	Thematic map indicating the probability of occurrence of submerged macrophytes

SOURCE: The Author (2022).

TABLE 3 - SUMMARIES OF SEVERAL APPLICABILITY STUDIES THAT MADE REMOTE SENSING USE

	STUDY	OBJECTIVE	STUDY AREA	SATELLITE	PERIOD	BANDS	SPECTRAL INDEXES	CALCULATED VARIABLE
Various applicability	PAN et al., 2018	Assess the impacts of climate change on vegetation	Dunhuang Yangguan National Nature Reserve, China	Landsat 5 and 8	1988 and 2016	Nir and Red	NDVI	vegetation area
	WANG et al., 2018	Determine the maximum and minimum annual extent of the water surface	Middle Yangtze River Basin, China	Landsat 4, 5 and 8	1990 - 2017	Nir, Red, Swir and Green	NDVI, NDWI, and mNDWI	surface water area
	WU et al., 2019	Analyze the variation of water storage	22 lakes in the Tibetan plateau, Asia	MODIS and LEGOS	2001 - 2017	is not cited	-	Area of lakes and respective water levels
	WIELAND; MARTINIS, 2020	Quantify variations in surface water extent during the 2018 drought	Germany	Sentinel-2	2018	Red, Green, Blue, Nir, Swir 1 and Swir 2	-	surface water area
	JAVED et al., 2020	Investigate spatio-temporal variations of drought	Different ground covers in China	MODIS	1982 - 2017	Nir and Red	NDVI and VCI and SPI	Indexes
	SUR et al., 2015	Compare conventional and remote drought sensing data	South Korea	MODIS	2004 - 2013	is not cited	-	EWDI and stMOD_ESI which are dry indices
	YAN; LIU; CHEN, 2018	Assess the reliability of precipitation products coming from the Tropical Rainfall Measuring Mission (TRMM)	China	TRMM	1998 - 2013	Precipitation	-	Precipitation

SOURCE: The Author (2022).

TABLE 4 - SUMMARIES OF STUDIES LINKED TO WATER QUALITY PARAMETERS USING REMOTE SENSING

	STUDY	OBJECTIVE	STUDY AREA	SATELLITE	PERIOD	BANDS	SPECTRAL INDEXES	CALCULATED VARIABLE
Water quality parameters	DEZORDI et al., 2015	Identify the bands that present the best response in the identification of turbidity	Part of Itaipu lake, Brazil	Landsat 8	09/08/2015	Blue, Green, Red, Nir, Swir 1 and Swir 2	-	Band-to-band ratio (for correlation with turbidity data)
	JIANG et al., 2019	Develop improved algorithm to obtain Secchi disk depth	8 lakes in Japan and US coastal waters	MERIS	2003 - 2012	is not cited	-	Secchi disk
	SCHAEFFER et al., 2018	Validate the use of temperature data from satellites	35 lakes and reservoirs and 24 estuaries in the US	Landsat 5 and 7	1980 - 2015	thermal data	-	water surface temperature
	LOBO et al., 2021	Develop platform to quickly obtain data on algal blooms	Reservoirs in Sao Paulo, Brazil	Sentinel-2	2015 - 2020	Red and Red Edge	NDCI	Normalized Difference Chlorophyll-a Index (NDCI)
	MARTINE et al., 2005	Assess water quality by satellite imagery comparing with field campaigns	Stretch of the Amazon River, Brazil	MODIS and MERIS	2003 - 2004	is not cited	-	Total suspended sediment, chlorophyll-a and organic matter
	PHILIPSON et al., 2016	Check whether satellite data can complement water quality monitoring	Lake Vanern, Sweden	MERIS	2002 - 2011	is not cited	-	Chlorophyll-a, dissolved organic matter, total suspended matter
	WATANABE et al., 2018	Check the performance of using band ratios to estimate chlorophyll	Barra Bonita Reservoir, Sao Paulo, Brazil	Landsat 8 and Sentinel-2	2014 - 2015	is not cited	2O, SLO, 2MSI, 3MSI, NDCI and SLMSI	Chlorophyll-a
	MENDES et al., 2022	Assess the potential of using long-term remote sensing imagery to detect and map potentially toxic elements in agricultural fields	Agricultural area in São Paulo, Brazil.	Landsat TM/ETM/ETM+, Landsat OLI and Sentinel 2.	1984 - 2019	All	-	Soil chromium, iron, nickel and zinc contents

SOURCE: The Author (2022).

TABLE 5 - SUMMARIES OF STUDIES LINKED TO MONITORING MACROPHYTES USING REMOTE SENSING

	STUDY	OBJECTIVE	STUDY AREA	SATELLITE	PERIOD	BANDS	SPECTRAL INDEXES	CALCULATED VARIABLE
Macrophytes	VILLA et al., 2018	Calibrate semi-empirical models to map morphological features of macrophytes	Lake Hidvegi, Hungary, and Lakes of Mantua, Italy	APEX	2014 - 2015	Blue, Green, Red, and Nir	27 indices	Fractional cover, leaf area index, and water biomass
	OYAMA; MATSUSHITA; FUKUSHIMA, 2015	Determine a method to distinguish cyanobacterial blooms and aquatic macrophytes	9 Lakes in Japan and 3 Indonesia	Landsat/TM and ETM+	Punctual images of the years: 1996, 2000, 2002, 2007, 2009 and 2011	Nir, Red and Swir	NDVI, five types of NDWI and FAI	Water area, cyanobacterial blooms and aquatic macrophytes.
	GALO et al. (2002)	Develop techniques for the assessment of the area with infestation of aquatic plants	Reservoirs in Sao Paulo, Brazil	ETM+/Landsat	2001	is not cited	-	Water and macrophyte area
	MESQUITA et al. (2013)	Quantify the existence of macrophytes	Umarí Dam, Rio Grande do Norte, Brazil	Landsat 5	2005 and 2006	Nir, Red and Green	-	Water and macrophyte area
	ROSA et al. (2017)	To verify if hydrological conditions of drought and rain had an influence on the dynamics of aquatic macrophytes	Banhado do Taim, Rio Grande do Sul, Brazil	Landsat/TM and ETM+	1984 - 2003	is not cited	-	Water and macrophyte area
	LIMA; LIBORIO; HADAD, (2018)	Identify sites with the presence of macrophytes, their attachment and accumulation points and analyze temporal changes	Rio Paraiba do Sul, Brazil	GeoEye-1	2010 and 2014	All	-	macrophyte area
	COLADELLO et al. (2020)	To verify the temporal and spatial evolution of the cover of aquatic macrophytes	Salto Grande Reservoir, Sao Paulo, Brazil	Landsat 5, 7 and 8	1984 to 2017	Nir and Red	NDVI	macrophyte area
	R&D 10381-0317	Develop methodologies for monitoring aquatic macrophytes in reservoirs	Jupiá Reservoir, Brazil	Sentinel-2	2017-CURRENT	Blue, Green, Red, Red Edge 1, Red Edge 2, Red Edge 3, Nir, Red Edge 4 and Swir	NDWI, NDVI, GNDVI, GSAVI, FAI	macrophyte area

SOURCE: The Author (2022).

TABLE 6 - SUMMARIES OF STUDIES LINKED TO REMOTE SENSING USING THE GOOGLE EARTH ENGINE (GEE)

	STUDY	STUDY OBJECT	STUDY AREA	SATELLITE	PERIOD	BANDS	INDEXES	CALCULATED VARIABLE
GEE	LI et al. (2021)	Retrieve the series of open surface water areas	Lake Chad (Chad, Cameroon, Niger and Nigeria)	AVHRR, Landsat, and MODIS	1980 - 2020	Nir and Red	NDVI	Water surface area and total inundated area
	WANG et al. (2018)	Determine the maximum and minimum annual extent of the water surface	Middle Yangtze River Basin, China	Landsat 4, 5 and 8	1990 - 2017	Nir, Red, Swir and Green	NDVI, NDWI, and mNDWI	surface water area
	Chen et al 2017	Assessing the potential of Landsat 8 imagery in annual glacial lake mapping	Tibet plateau, Asia	Landsat 8	2015	Green and Swir	mNDWI	Spatial distribution of lakes
	Fang et al 2019	Assess the variation in water storage	760 lakes and reservoirs in China	Landsat 5, 7, and 8	1984 - 2015	is not cited	-	surface water area
	Uddin et al 2019	Develop an operational methodology for flooding and mapping potentially flood-damaged areas	Bangladesh, India	Sentinel-1 and Landsat 8	2017	Nir, Red and Swir	NDVI and NDWI	flooded area
	Xiong et al 2021	They evaluated the spatio-temporal variations and spatial autocorrelation of ecological quality	Lake Erhai, China	Landsat 5 and 8	1999, 2004, 2009, 2014 and 2019	Blue, Green, Red, Nir, Swir 1 and Swir 2	NDVI, WET, NDSI, mNDWI and LST	Correlations between indices
	LOBO et al., 2021	Develop platform to quickly obtain data on algal blooms	Reservoirs in Sao Paulo, Brazil	Sentinel-2	2015 - 2020	Red and Red Edge	NDCI	Normalized Difference Chlorophyll-a Index (NDCI)
	This dissertation	**Spatio-temporal variation of aquatic macrophyte cover in a reservoir using landsat images and google earth engine**	**Jupiá Reservoir, Brazil**	**Landsat 5, 7, and 8**	**1984-2021**	**Nir, Red and Green**	**NDVI, GNDVI and GSAVI**	**Macrophyte area and correlations**

SOURCE: The Author (2022).

3 MATERIAL AND METHODS

Initially in this chapter, the characteristics of the study area will be described – the reservoir of Engenheiro Souza Dias HPP, also known as Jupiá. This region is target of a research project in progress (Research and development project - P&D ANEEL 10381- 0819/2019), by Lactec and the concessionaire that manages and operates the Engenheiro Souza Dias HPP, CTG Brasil, related to the development of an Emergencies Action Plan for Macrophytes. It is noteworthy that the activities developed in this dissertation are included in this P&D ANEEL project.

This study follows on from another P&D project (nº 10381-0317 - Monitoring the development and displacement of aquatic macrophyte banks in reservoirs using geotechnologies and remote sensing techniques). Together, of the numerous products developed in these two studies, we can mention the diagnosis of water quality and a floristic survey, through onside collections (LACTEC, 2019b), a Macrophyte Monitoring System through remote sensing, which was implemented to an alert system (LACTEC, 2019c) currently used by the concessionaire in the HPP operation, in addition to the determination of critical locations for monitoring through the spatial analysis of macrophyte permanence (LACTEC, 2020).

Afterwards, the procedures and criteria used to identify aquatic macrophytes in satellite images are presented, as well as information on the set of images used. Finally, the chapter ends with a description of the methodology used to construct macrophyte cover permanence curves and how environmental and operational variables will relate to the macrophyte area historical series.

3.1 STUDY AREA DESCRIPTION

Formed in 1968 by the damming of the Paraná, Tietê and Sucuriú Rivers (FIGURE 5), the Jupiá reservoir has a storage volume of 904 hm^3, spread over 330 km^2 with 482 km perimeter and it is located between São Paulo and Mato Grosso do Sul states (Mustafa et al., 2010). Its main use is power generation at the Engenheiro Souza Dias HPP, which operates as a run-of-the-River reservoir with constant power generation, with an average annual water residence time of 6.39 days (CESP, 2009). The water level near the dam (altitude of 229 m) remains on average at 279.6 m, with minimum depletions of ± 0.50 m, and as a consequence, there is no formation of

intermittent ponds. Besides, a significant part of the reservoir has depths of around 3.50 m and reaches up to 45 m in a small branch of the Paraná River.

FIGURE 5 - LOCATION, SOME OF THE MACROPHYTE SPECIES FOUND AND THE DEPTH OF THE JUPIÁ RESERVOIR.

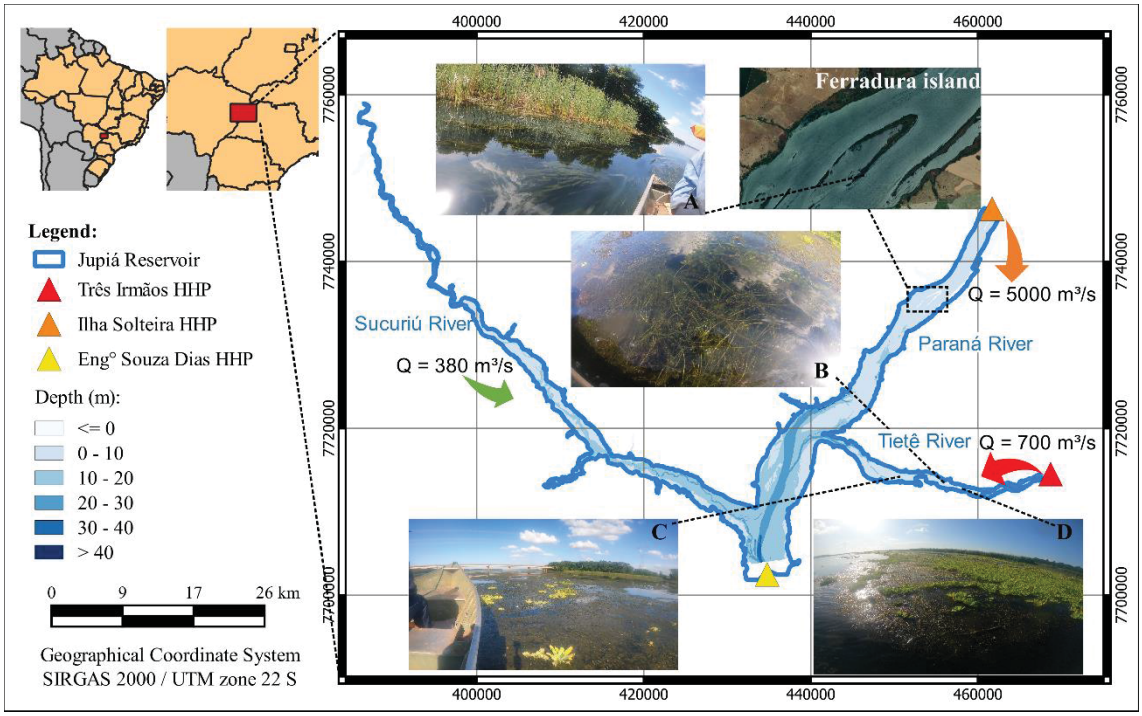

SOURCE: The Author (2022).

LEGEND: (A): field research photographic records (04/05/2022) of *Egeria densa* and *Typha domingensis* near Ferradura island, in the Paraná River; (b): field research photographic records (04/06/2022) of *Egeria densa* and *Egeria najas* upstream of the Tietê River bridge, on the Tietê River; (c): field research photographic records (04/06/2022) of *Egeria densa, Egeria najas* and *Pistia stratiotes* downstream of the Tietê River bridge, on the Tietê River and; (d): field research photographic records (04/06/2022) of *Egeria densa*, *Egeria najas* and *Pistia stratiotes* upstream of the Tietê River bridge, on the Tietê River.

The climate in the region is tropical savannah (Aw), according to the Köppen-Geiger classification. The region has an average annual rainfall of around 1200 mm, with rainy Summers and dry Winters (FIGURE 6), with an average annual temperature of 24°C.

Jupiá's water quality is characterized by high water transparency, in which in some regions it is possible to see the Riverbed even at depths of 3 to 5 m (total Secchi Disk). Regarding the amount of nutrients available, it was observed that phosphorus was the limiting element in most of the monitored period (2018-2019). Concentrations above 0.050 mg/L (class 2 freshwater limit by CONAMA resolution nº 357/2005) were

found in 4 of the 6 campaigns carried out, with the highest value of 1.56 mg/L on Ferradura Island in December/2018. As for total nitrogen concentrations, in no sample the legislated limits for fresh waters of Classes 1 and 2 (2.18 mg/L) were exceeded (LACTEC, 2019b).

Due to these characteristics, the Jupiá reservoir has an abundant occupation of aquatic macrophytes that can detach and move to the dam following the flow. This amount is so expressive that in 2017, this phenomenon was responsible for stop the energy generation due to the clogging of the water intake structures (CTG Brasil, 2019).

LACTEC (2019a) carried out a floristic survey in which the species of aquatic macrophytes with the highest occurrence were identified (Egeria densa, Egeria najas and Typha domingensis (FIGURE 5) and the characteristic of the place where they were found. Free submerged species were found on the banks, and submerged ones rooted in the central area of the reservoir. The floating and rooted ones were found in more protected areas, such as shores and ponds.

FIGURE 6 - AVERAGE MONTHLY INFLOWS[1] INTO THE JUPIÁ RESERVOIR BETWEEN 1984-2021; ANNUAL AND MONTHLY PRECIPITATION BETWEEN 1984-2021[2] AND AVERAGE MONTHLY TEMPERATURE[3] AT ILHA SOLTEIRA STATION BETWEEN 1991-2021

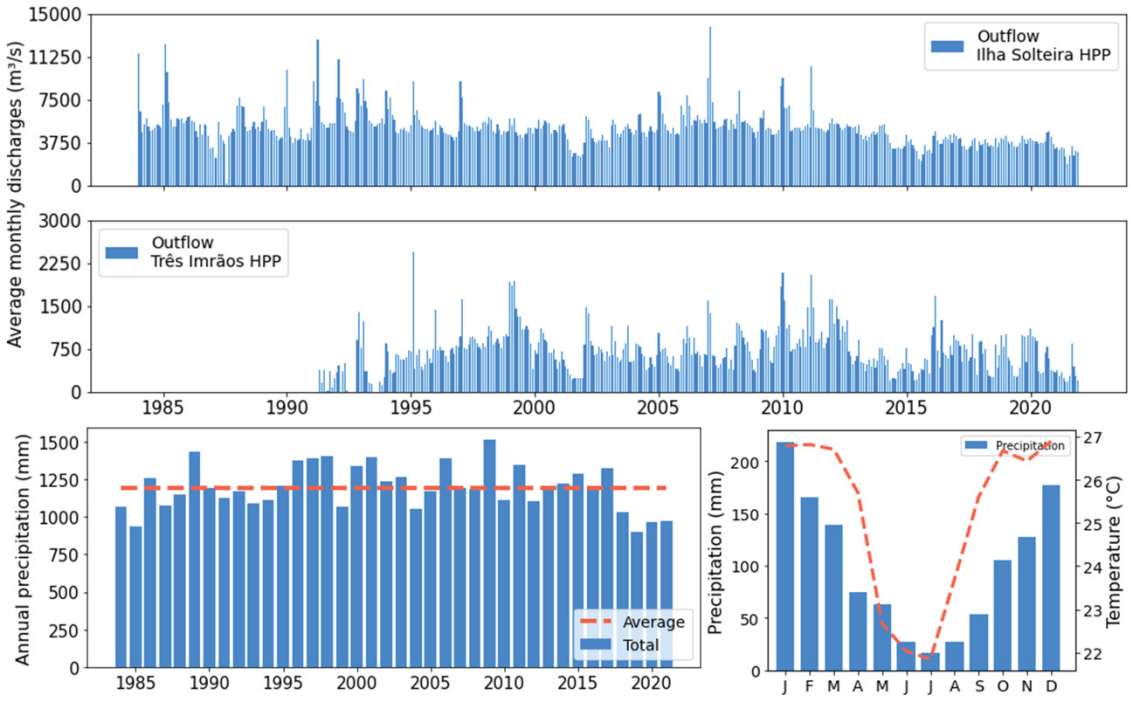

SOURCE: CTG Brasil (2022) [1], CHIRPS (2022) [2] e UNESP (2022) [3].

3.2 MACROPHYTES IDENTIFICATION IN LANDSAT IMAGES

The macrophyte identification procedure in the satellite images consisted of 14 steps (FIGURE 7) and the use of images from the USGS Landsat 5, 7 and 8 collections (Collection 2, Level 2), orbit 223 (WRS PATH), which have spectral resolution of 30 m and with previous atmospheric surface reflectance corrections (BoA) by the TM, ETM+ and OLI/TIRS sensors, respectively. Since the aim is the historical knowledge of the region, preference was given to these collections over other options due to the interval of data availability being over 30 years. These images were processed using the Google Earth Engine – GEE (Google, 2022) due to the wide catalog of satellite images and, mainly, because the processing is carried out in the Google cloud, which enables the use of many images, since downloading them is not necessary. It should also be noted that the R-4.1.3 and Python 3.9.7 languages were used for statistical analysis and data visualization.

FIGURE 7 - AQUATIC MACROPHYTES CLASSIFICATION PROCESS FLOWCHART IN LANDSAT 5, 7 AND 8 IMAGES.

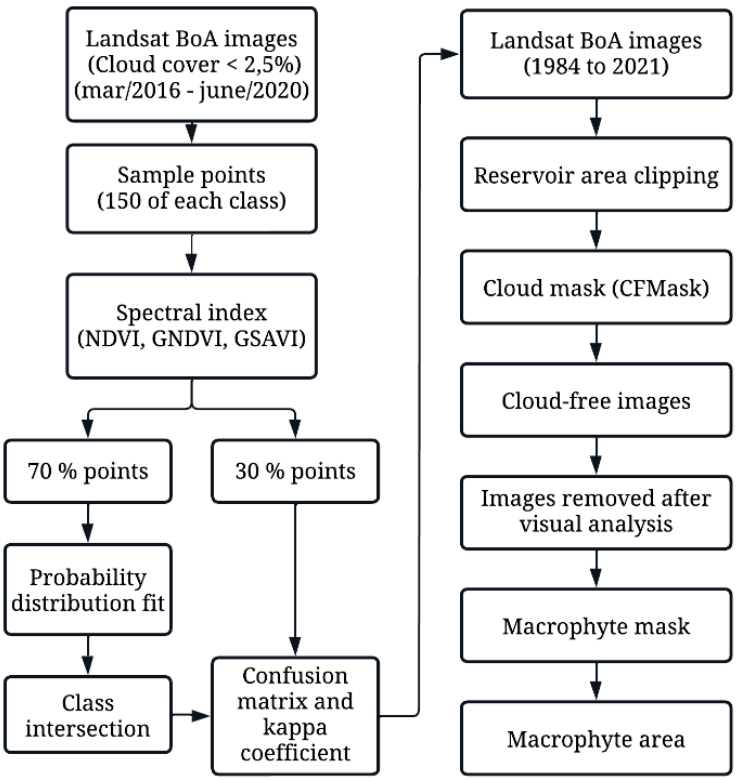

SOURCE: The Author (2022).

Initially, images from March/2016 to June/2020 that had cloud cover up to 2.5% were selected for the insertion of sample points of three classes: water, macrophyte and “other vegetation”. This procedure was carried out with the objective of verifying the limit of the separation between the classes in the spectral indices.

Cloud cover was limited in order to reduce data interference. The time period used coincides with data compiled in maps of permanence (in regions with probability of occurrence of water, macrophytes and other vegetation) reported in (LACTEC, 2020).

Thus, of the 65 images available, after a visual analysis, 32 were discarded due to the failure of the ETM+ sensor and 6 due to cloud interference in the reservoir region. In all, 27 images were considered suitable for use, and different sets of samples were inserted in each of them: 150 water points, 150 of macrophytes and 150 of other vegetation; based, in addition to the analysis of macrophyte permanence (LACTEC, 2020), field photographic records (FIGURE 8). These known sampling points were used as input in a supervised classification. As the study area is limited to the reservoir, in addition to the differentiation between water and macrophytes, it was considered convenient to distinguish between macrophytes and other vegetation, the latter presented and fixed on islands inside the reservoir (FIGURE 9).

To verify the boundaries between classes, for each class, from 4050 points (150 points in 27 images), 70% were randomly selected to observe the frequency of the spectral indices NDVI, GNDVI and GSAVI and in the bands that compose them: Red (0.63 to 0.69μm), Green (0.52 to 0.60μm) and Nir (0.77 to 0.90μm). To these data, it was verified which probability distribution would best fit the sample of each class, considering the result of the Anderson-Darling adherence test, in order to verify the limit values that characterize the class of macrophytes. This test is used to check whether a data set comes from or belong to a certain probability distribution (NAGHETTINI; PINTO, 2007).

The best index-interval was defined through a validation, in which, with the remaining 30% of points, the confusion matrices and the Cohen's kappa coefficient (LANDIS; KOCH, 1977) (TABLE 7) of each model were calculated.

FIGURE 8 - FIELD RESEARCH PHOTOGRAPHIC RECORDS AND DETAILS OF WATER, AQUATIC MACROPHYTES AND OTHER VEGETATIONS SAMPLE POINTS

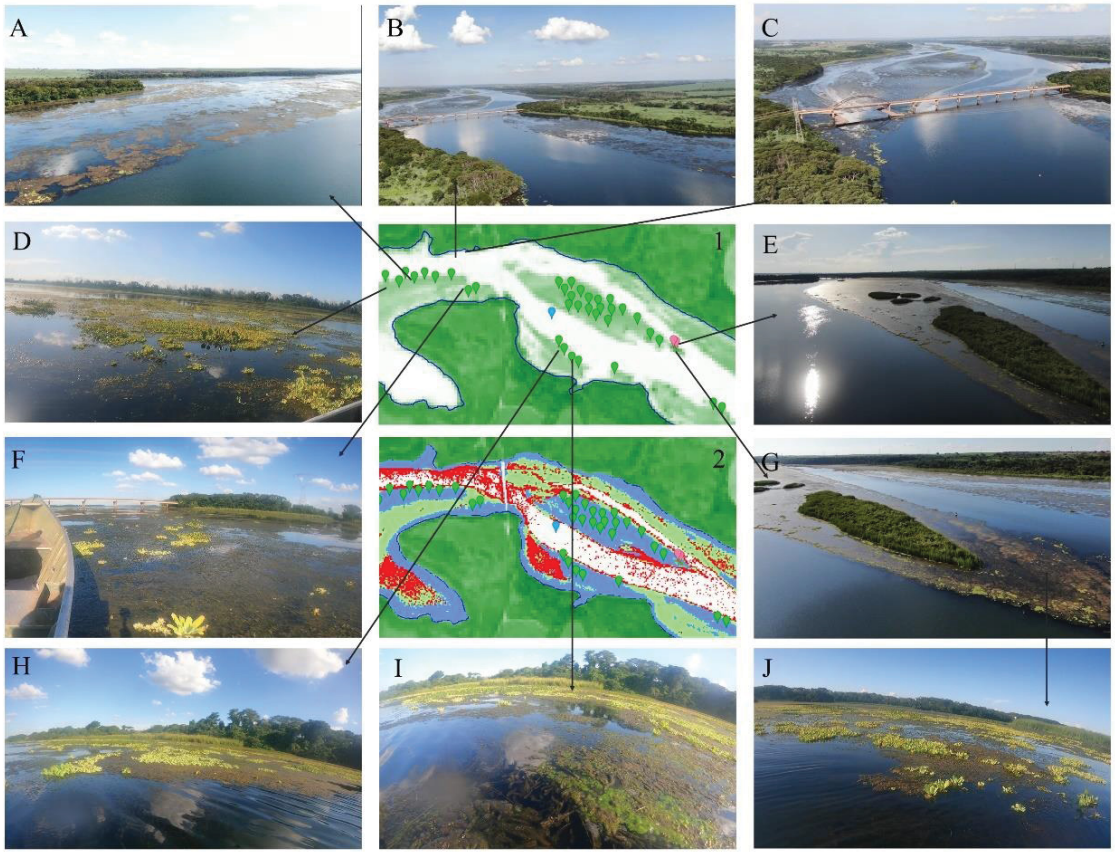

SOURCE: The Author (2022).

LEGEND (1): GSAVI Landsat image (03/05/2017) of the Tietê River region with the sampling points; (2): GSAVI Landsat image (03/05/2017 of the Tietê River region with the macrophyte permanence areas (LACTEC, 2020) in which red represents low permanencies, green represents intermediaries permanencies, blue represents high permanencies and white areas without macrophytes, and; (A, B, C, D, E, F, G, H, I, J): Field research photographic records (06/04/2022).

FIGURE 9 - VEGETATION AND PERMANENT SETTLEMENT DETAILING AT FERRADURA ISLAND, ON PARANÁ RIVER.

SOURCE: The Author (2022).

LEGEND (1): (A): GSAVI Landsat image (03/05/2017) from the Ferradura island region, on the Paraná River with the sampling points in which pink points represents vegetation and green points macrophytes; (B): CNES image (Google Earth Engine, 2022) Vegetation and permanent settlement detailing at Ferradura island, on Paraná River and; (C): Ferradura island field research photographic with large vegetation fixed to the ground and *Typha domingensis* in the water (05/04/2022).

After defining the best index and range for macrophyte identification, all images between the years 1984 and 2021 (597 images) were clipped, in order to encompass only the representative polygon of the reservoir area to the height 280 m (operational quota), and a cloud mask was applied to select only cloud-free images. Images that met this condition (179 images) underwent a visual analysis and it was necessary to discard the images which presented interference due to the sunlight (5 images), by the attenuation of the color (30 images) and images that did not contemplate the entire reservoir (2 images) (FIGURE 10). Next, a macrophyte mask was applied to the remaining images (142 images), so that the macrophyte area was calculated by counting pixels.

TABLE 7 - COHEN'S KAPPA COEFFICIENT REFERENCES.

Kappa	Strength of Agreement
≤ 0,00	Poor
0,01 - 0,20	Slight
0,21 - 0,40	Fair
0,41 - 0,60	Moderate
0,61 - 0,80	Substantial
0,81 - 1,00	Almost Perfect

SOURCE: Adapted from Landis & Koch (1977, p. 165).

FIGURE 10 - EXAMPLE OF ERRORS PRESENT IN IMAGES WHICH WERE DISCARDED AFTER VISUAL ANALYSIS

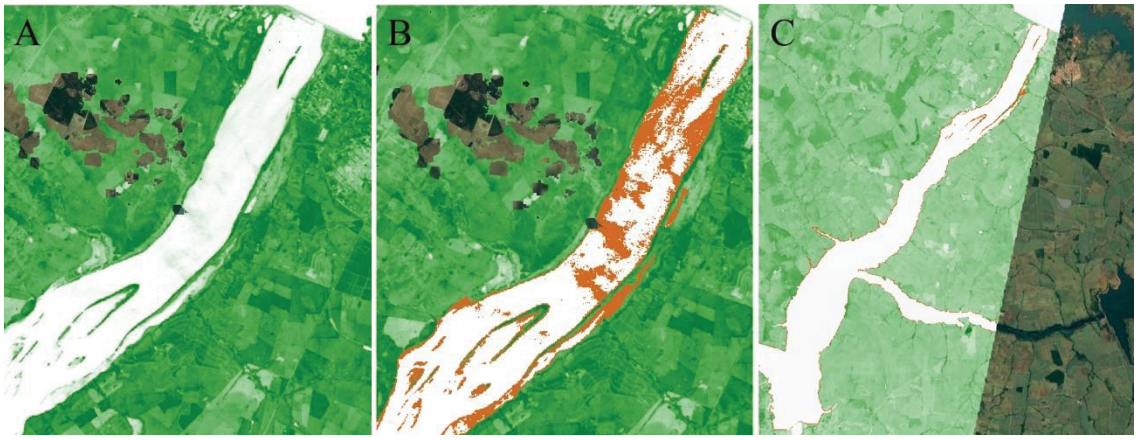

SOURCE: The Author (2022).

LEGEND (A): GSAVI Landsat image (24/11/2010) with sunlight interference in the northern region of the Paraná River; (B): GSAVI Landsat image (24/11/2010) with erroneous macrophytes classification due to sunlight interference in the northern region of the Paraná River, and; (C): GSAVI Landsat image

(28/08/1984) which did not contemplate the entire region of the Jupiá reservoir, in addition to presenting a more attenuated color (shades of green) in comparison to A.

3.3 CURVES AND MAPS OF MACROPHYTE AREA PERMANENCE

After calculating the area of macrophytes in each image, a permanence curve was calculated by ordering the values in descending order and calculating the frequency, using Kimbal's method. In this method the frequency is calculated so that the denominator is the sum of the sample size plus 1.

Additionally, by mapping the spatial distribution of macrophytes in each image, the permanence of macrophytes in each pixel was calculated. This could be done because the macrophyte classification returns a binary result of the presence or non-presence of macrophyte in each pixel. The procedure was performed using the 'raster calculator' tool of QGIS 3.16.16-Hannover software, through the sum of all macrophyte masks and frequency calculation was also done by the Kimbal method.

In both analyses, in addition to observing the complete series, the data were also grouped seasonally, to verify if there were interannual variations, and also by decades to evaluate.

3.4 ENVIRONMENTAL VARIABLES EFFECTS ON MACROPHYTE GROWTH

There are some physical and environmental characteristics that influence the growth of macrophytes for example the availability of nutrients (both those disposed in the sediment and those dissolved in the water), the availability of light (which in turn depends on factors such as incident solar radiation and water turbidity), temperature (as it acts as a catalyst in photosynthetic processes), hydrodynamic and hydrological conditions (either by the variation of levels or by the speed of current, such as by the rainy and dry seasons), and also the action of predators (BIANCHINI JUNIOR, 2003; ESTEVES, 1998; TUNDISI; TUNDISI, 2008).

One of the indirect ways of verifying changes in nutrient availability is through changes in land use, since the increase in human activities, such as urbanization and agriculture, is a factor that can cause eutrophication of water bodies. To investigate this phenomenon, the watershed of the Jupiá reservoir was delimited (considering the dam as an outlet), and the incremental areas of each contribution from the reservoir

were also calculated: Sucuriú River (considering the beginning of the reservoir as an outlet) and the reservoirs of Ilha Solteira and Três Irmãos (both considering the dam as an outlet for the basin). In these areas, changes in land use were verified with MapBiomas data over the years 1985-2020, also through the GEE platform.

As there is no variation in Jupiá level, to verify the influence of the reservoir hydrodynamics on the macrophytes growth, the average monthly outflows of the upstream plants of Jupiá (Ilha Solteira HPP and Três Irmãos HPP) were analyzed, while, to assess the influence of climatological conditions, temperature and precipitation were analyzed.

4 RESULTS AND DISCUSSIONS

The results will be presented below according to the disposition of the methodology. First, the best index and its respective range will be defined for the classification of macrophytes in the images. Next, the macrophyte area historical series and seasonality analyzes will be illustrated, as well as the permanence curves for each season and for each decade covered. In the same way, the maps of permanence will also be presented. As a conclusion, it will be exposed how the macrophytes historical series was related to changes in land use, precipitation and temperature, and also to the operation of HPPs upstream of the Jupiá reservoir.

4.1 MACROPHYTES IDENTIFICATION IN LANDSAT IMAGES

To verify the boundary between the classes (water, macrophyte and vegetation), the 70% of sampling points frequency of the NDVI, GNDVI and GSAVI spectral indices were analyzed, in addition to the bands that compose them: Red, Green and Nir (FIGURE 11).

In the histograms, it can be seen there was a massive overlap from three classes for Green, while for Red, the overlap was not so great between the macrophyte and vegetation classes, although it still exists. For the Nir band, the overlap was smaller when compared to the visible bands (Green and Red).

The values recorded in the water class correspond to the spectral behavior expected by this class: great absorption of Nir radiation and low reflectance in the

visible bands (NOVO, 1989); which implies negative and close to zero values of the analyzed indices (GITELSON et al., 1996; HUETE, 1988; ROUSE et al., 1973).

FIGURE 11 - FREQUENCY DIAGRAMS OF RED, GREEN AND NIR BANDS, AND NDVI, GNDVI AND GSAVI SPECTRAL INDICES CONSIDERING 70% OF THE WATER, MACROPHYTE AND OTHER VEGETATION DATA.

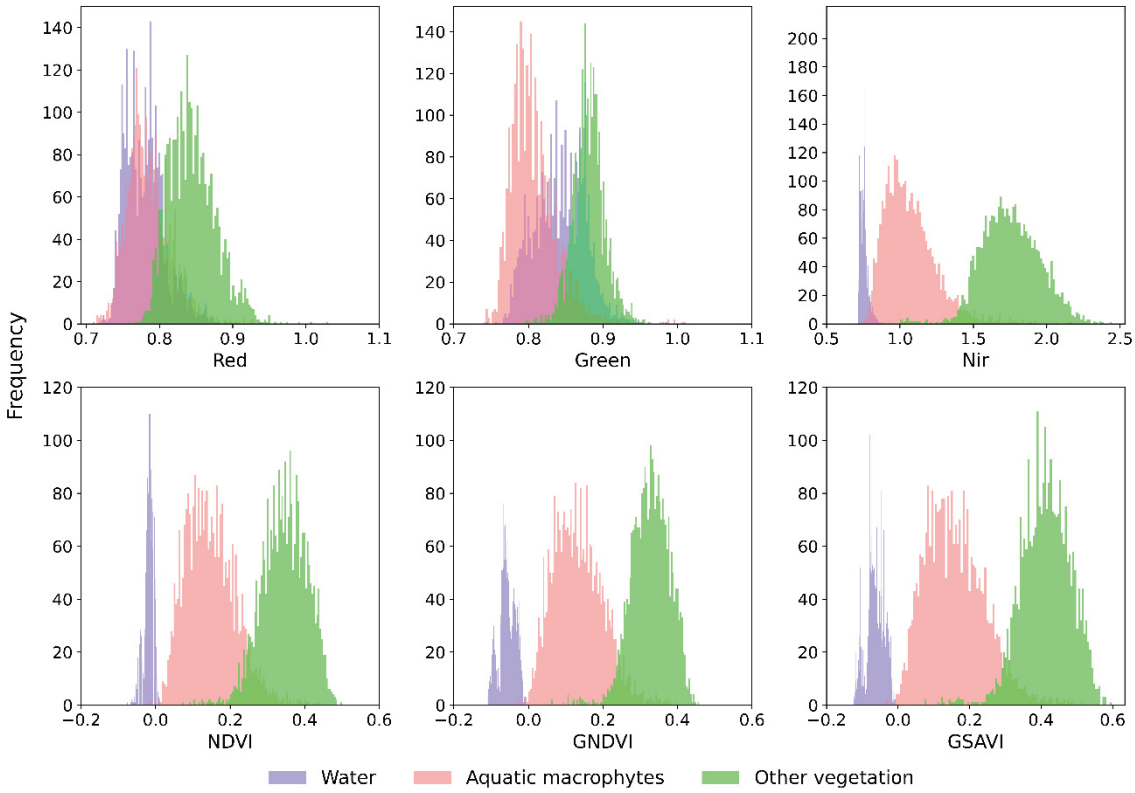

SOURCE: The Author (2022).

The macrophytes and other vegetation values followed the general behavior of vegetation: they reflect a lot of Nir radiation and little of visible radiation; which implies positive values for the analyzed indices (GITELSON et al., 1996; HUETE, 1988; ROUSE et al., 1973). The difference between these classes may be in the color of each species (Red) as well as in the water interference on macrophytes (NOVO, 1989).

For the three spectral indices, it was possible to observe an overlap between the macrophyte and other vegetations classes and a distinct separation between the water and macrophyte classes, which is the reason why only the intersection between the macrophyte classes and other vegetations was verified. With these data, for each index, 16 probability distributions were adjusted and the value of the Anderson-Darling (AD) adherence test (NAGHETTINI; PINTO, 2007) was evaluated. For all indices, of

the curves tested with data from other vegetations, none showed an acceptable p-value (p-values < 0.05), while for macrophytes data, only the 3-parameter Weibull distribution met the test (p -value = 0.073). Anyway, it was found that in the region of intersection between the classes, both macrophytes and other vegetation data can be approximated by a normal distribution (FIGURE 12).

FIGURE 12 - FIT OF MACROPHYTE AND OTHERS VEGETATION DATA TO NORMAL DISTRIBUTIONS.

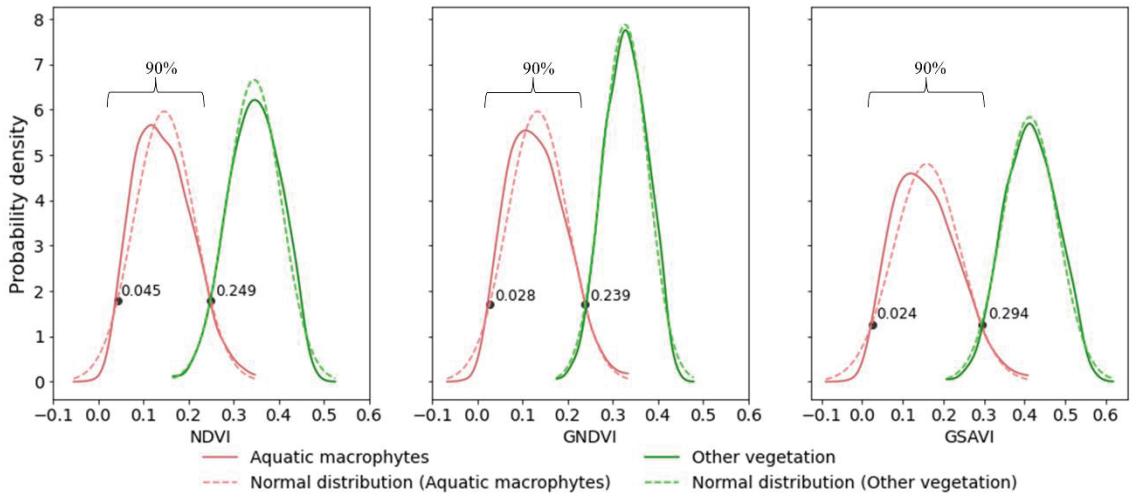

SOURCE: The Author (2022).

LEGEND: the upper limit of each index was obtained at the point where the probabilities of the curves were equal, and the lower limit was determined at the value where 90% of the data were encompassed.

Thus, for each index, the upper limit of the macrophyte class was determined from the value where the macrophyte classes and other vegetations PDF curves (probability density function) coincided. The macrophyte class lower limit was given by the PDF curve, in order to encompass 90% of the data, based on the value of the upper limit. With the limits of each index determined, to find out which index-interval set presented the best behavior, the 30% remaining points of each class were used to calculate the confusion matrix and the Kappa coefficient.

It was observed that three index-interval sets presented high values for the Kappa coefficient (TABLE 8), being the use of any of them very satisfactory for aquatic macrophytes identification in Landsat images (LANDIS; KOCH, 1977).

Therefore, the GSAVI index-interval set (0.024 to 0.294) was adopted, because its kappa result's was superior to the others. For the water classification, all values below 0.024 were considered, while for other vegetation, all values above

0.294. For instance, two images were selected - being: one before (FIGURE 13) and another after the May/2017 event (FIGURE 14) – in which it is possible to notice the macrophytes cover change in the region of the Paraná River, and of even more substantially on the Tietê River.

TABLE 8 - AQUATIC MACROPHYTE CLASSIFICATION CONFUSION MATRICES AND MODEL ACCURACY

Index		NDVI (0.045 – 0.249)			GNDVI (0.028 – 0.239)			GSAVI (0.024 – 0.294)		
Actual		W[1]	A.M.[2]	O.V.[3]	W	A.M.	O.V.	W	A.M.	O.V.
Predicted Class	W	1,252	0	0	1,252	0	0	1,252	0	0
	A.M.	0	1,169	71	0	1,173	41	0	1,176	37
	O.V.	0	71	1,181	0	67	1,211	0	64	1,215
Kappa		**0.962**			**0.971**			**0.973**		

SOURCE: The Author (2022).

LEGEND: W[1] = Water; A.M.[2] = Aquatic Macrophyte and; O.V.[3] = Others Vegetation.

FIGURE 13 - AQUATIC MACROPHYTES IDENTIFICATION IN THE LANDSAT 8 IMAGE FOR 03/05/2017.

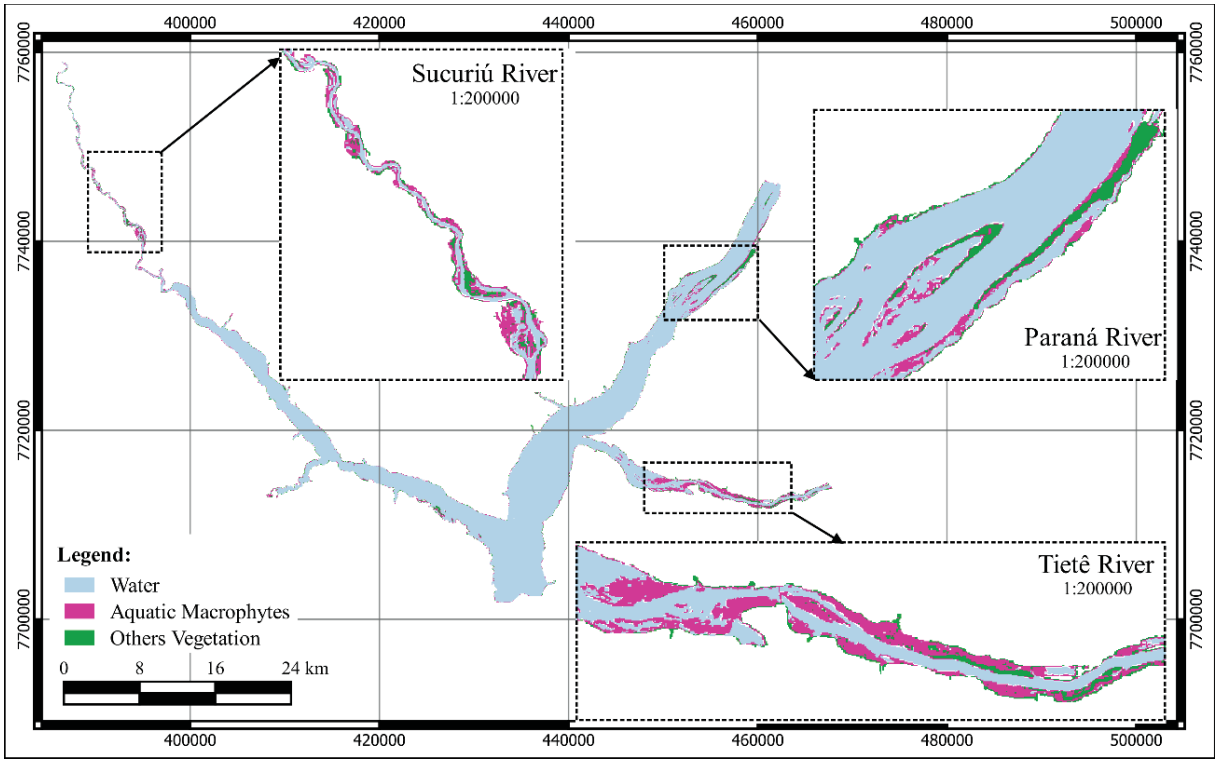

SOURCE: The Author (2022).

FIGURE 14 - AQUATIC MACROPHYTES IDENTIFICATION IN THE LANDSAT 8 IMAGE FOR 06/07/2017.

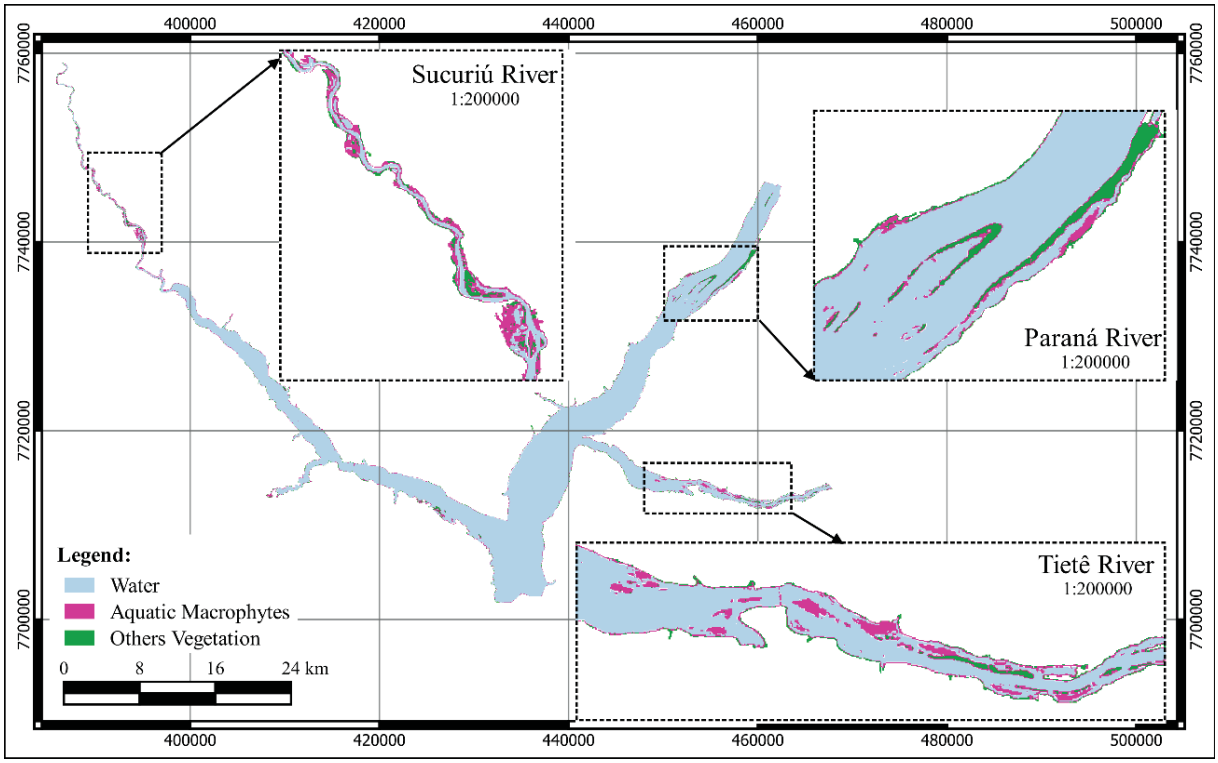

SOURCE: The Author (2022).

4.2 MACROPHYTE AREA HISTORICAL SERIES

Between 1984-2021, 142 images were considered able for use. These images are heterogeneously distributed over time (TABLE 9), since in 2003, 2011, 2012 and 2013 there were no appropriate images, also there are different amounts of images between years, and in a year, between seasons.

Macrophytes identification in these images was performed by applying the macrophyte mask using the GSAVI index (0.024-0.294), while the area was determined by counting pixels. It was possible to notice a growth trend (stationarity hypothesis rejected) with the advancement of time (FIGURE 15), in which, by adjusting a linear trend ($R^2 = 0.41$) the growth rate is 4.55 10^{-4} km²/day. The highest recorded area value was 26.57 km² on 12/21/2020 (8% of the reservoir area) while the smallest mapped area was on 03/14/1987 with 10.52 km² (3% of the reservoir area), accumulating a difference of more than 50%. The average area observed throughout the period was 16.83 km² (5% of the reservoir area). Other authors who used similar methodologies, and Landsat set images, also observed growth over the analyzed

period (COLADELLO et al., 2020; LIMA et al., 2018; LUO et al., 2016; MINHONI et al., 2017, 2018).

TABLE 9 - QUANTITY AND TEMPORAL IMAGES DISTRIBUTION USED TO COMPOSE THE MACROPHYTE COVERAGE TIME SERIES BETWEEN 1984-2021.

Year	84	85	86	87	88	89	90	91	92	93	94	95	96	97	98	99	00	01	02	03	04	05	06	07	08	09	10	11	12	13	14	15	16	17	18	19	20	21	Total
Total	1	5	3	6	5	3	3	5	1	5	1	3	2	1	2	3	4	6	4	0	3	5	2	6	7	3	2	0	0	0	6	4	7	9	4	7	6	8	142
Jan											1								1																					2
Feb					1																1													1		1			4
Mar		1		2			1											1							1										1	1	1		9
Apr						1				1			1		1		1	2	1		1			2	1	1					1	1	2	1			1	1	20
May				1	1			2		1		1					2	1	1			1			1						1			1	1		1		16
June			1	1		1	1	1				1							2		1	1		2		1	1							1		1	1	1	18
Jul	1	2			1		1			2				1			1	1					1		2		1				2		1	2		2		1	22
Aug		1	1	1								1						1				2		1	1						1	1	1	2	1		1	2	18
Sept					1	1																	1	1		1					1	2	1	1	1	1		2	14
Oct		1	1	1				1	1				1		1																		1			1			9
Nov					1			1		1											1																		4
Dec																1	1								1								1				1	1	6

Legend: Landsat 5 TM | Landsat 7 ETM+ | Landsat 8 OLI/TIRS | No data

SOURCE: The Author (2022).

With the seasonality analyses throughout the historical series, it was possible to notice that there were decrease in areas in Winter and Spring, while in Autumn there was an increase (FIGURE 15). Furthermore, until 1996, the largest areas occurred in Winter and/or Spring, however there was an inversion and since then these values have been recorded in Summer and/or Autumn. This is similar to what was described by Rosa et al. (2018) who found an increase in the area between March and April followed by a decrease between April and September in a branch of the Itaipu reservoir.

Likewise, from 2014 onwards, a greater number of elevated area is registered in Autumn, while smaller areas are registered in Winter, which could be a potential indicator that there is detachment and/or transport of macrophytes between these seasons

FIGURE 15 - MACROPHYTE COVERAGE AREA HISTORICAL SERIES FOR THE 142 IMAGES SELECTED USING GSAVI INDEX (0.024 - 0.294) AND PRESENTED BY SEASON.

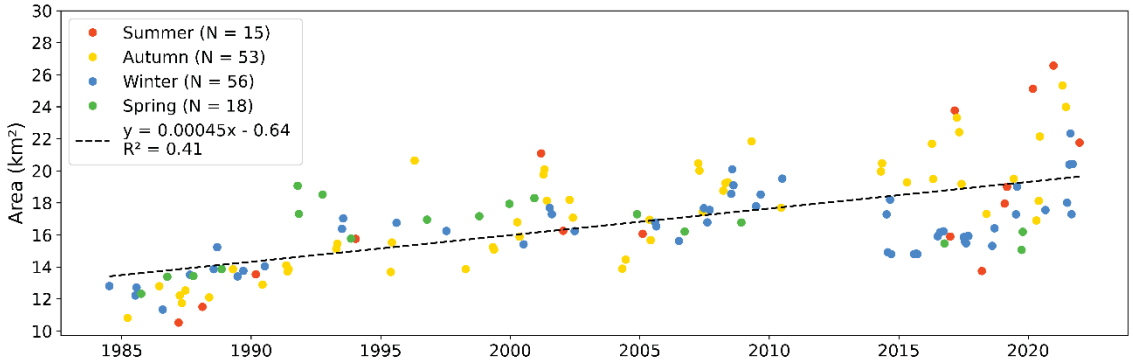

SOURCE: The Author (2022).

Furthermore, a growth trend over time it was also verified (stationarity hypothesis rejected) for the maximum and minimum values of each year. Curves were fitted for those data, which in, for the maximum annual area data, the fit was superior to the curve containing the complete series (FIGURE 16).

FIGURE 16 - MAXIMUM AND MINIMUM AREAS OF MACROPHYTES AND LINEAR TREND CURVE FIT.

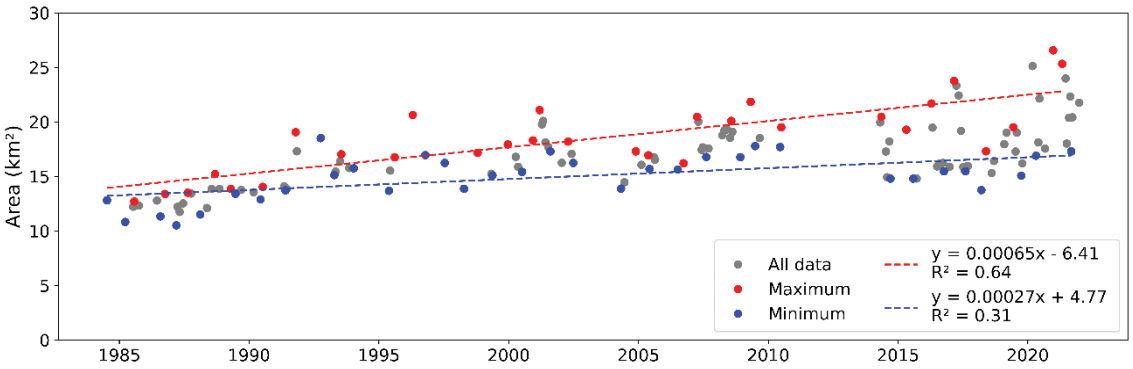

SOURCE: The Author (2022).

4.3 MACROPHYTE AREA PERMANENCE CURVE

Macrophyte area permanence curves were calculated for the entire period analyzed and seasonally, separating all data into distinct curves for each of the decades and for each season.

Considering the complete series, the data could be satisfactorily fitted by a polynomial of third degree ($R^2 = 0.98$) (FIGURE 17), although the maximum values were being underestimated. The curve showed a smooth behavior and similar to an S,

which implies that intermediate values have little variation between them, and more accentuated variations at the ends.

Observing the behavior over the decades, it is possible to see the areas increased over the decades, especially when it comes to areas with the highest macrophytes cover, that is, frequencies < 50% and at maximum values (FIGURE 17). For most of the time (frequencies > 50%), the 2000s presented values slightly higher than the 2010s, followed by the other decades in descending order. It is also noteworthy the curve of the 2010s was always higher than the historical series curve, corroborating the growth trend observed in the stationarity test.

FIGURE 17 - MACROPHYTE COVERAGE AREA PERMANENCE CURVES FOR EACH DECADE (1984-1989, 1990-1999, 2000-2009 AND 2010-2021), FOR THE ENTIRE HISTORICAL SERIES (1984-2021) AND ITS RESPECTIVE POLYNOMIAL ADJUSTMENT CURVE

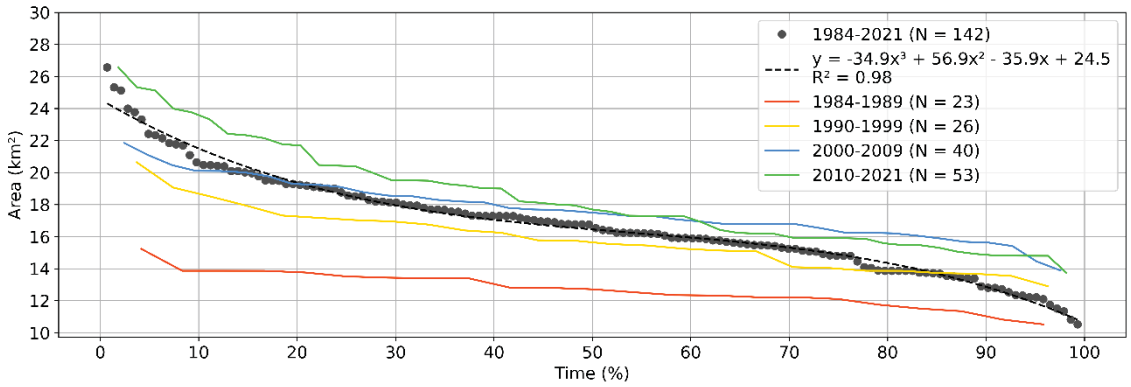

SOURCE: The Author (2022).

In addition, the area variation was greater (σ = 3.17 km²) in the 2010s, which is the broader curve than the others (FIGURE 18). The 1990s and 2000s had intermediate behavior and similar variations (σ = 1.92 km² and σ = 1.79 km², respectively), with the difference in the 2000s having values slightly higher than the previous one. Corroborating previous results, the 1980s were the decade that presented, besides the smallest variation (σ = 1.12 km²), the smallest minimum, average and maximum values.

FIGURE 18 - BOXPLOT OF THE MACROPHYTE AREAS VARIATION EACH DECADE

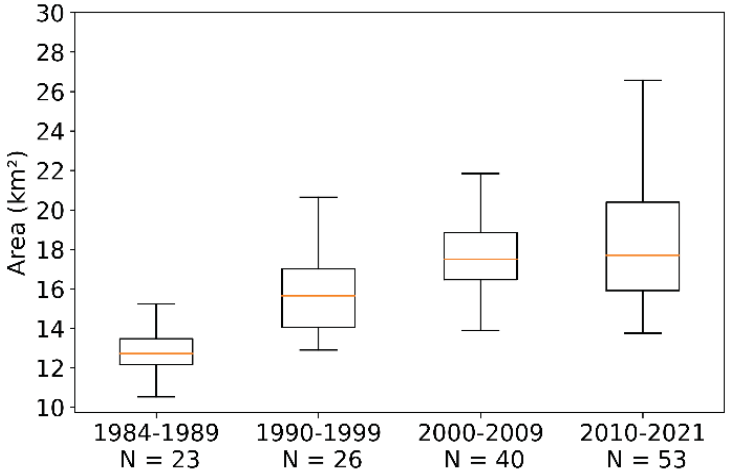

SOURCE: The Author (2022).

When it is analyzed seasonally, it can be seen again that the highest macrophyte areas were recorded in Summer and Autumn. In most of the analyzed time (84%), for all seasons, the occupancy area was greater than 14 km² (4% of the reservoir area), and in 50% of the time the macrophyte occupancy area remained between 16 and 18 km² (FIGURE 19). This curve overlapping in the highest frequency region could may be a reflection of area variation between the seasons being smaller in the first half of the series (1985-2005) when compared to the final period (2005-2021).

The season that presented the greatest dispersion of values (σ = 4.89 km²) was the Summer, which englobe the historical series of maximum and minimum values, with an amplitude of 16.05 km². Spring was the season with the lowest data amplitude (σ = 1.93 km²) (FIGURE 20), with the difference between its extreme values being 6.74 km². It is noteworthy that Summer and Spring were the seasons that presented about 3.5 times less images than Autumn and Winter, as the presence of clouds was the limiting factor, due to greater precipitation in this period (FIGURE 6). This limitation was already expected as a consequence the interference of clouds in the optical sensors of orbital satellites and was a common factor for the image's quantity used in several other studies (COLADELLO et al., 2020; ROSA et al., 2018).

FIGURE 19 - MACROPHYTE COVERAGE AREA PERMANENCE CURVES FOR EACH SEASON (SUMMER, AUTUMN, WINTER AND SPRING), FOR THE ENTIRE HISTORICAL SERIES (1984-2021) AND ITS RESPECTIVE POLYNOMIAL ADJUSTMENT CURVE.

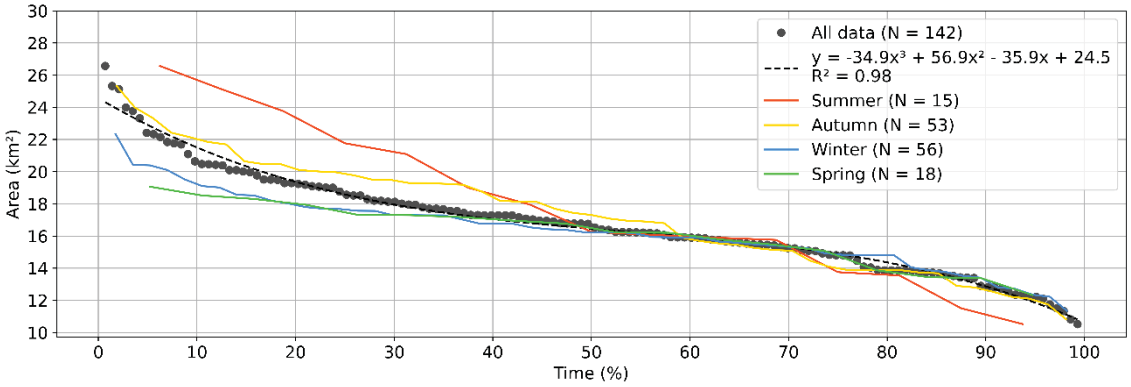

SOURCE: The Author (2022).

FIGURE 20 - BOXPLOT OF THE MACROPHYTE AREAS VARIATION IN EACH SEASON OF THE YEAR.

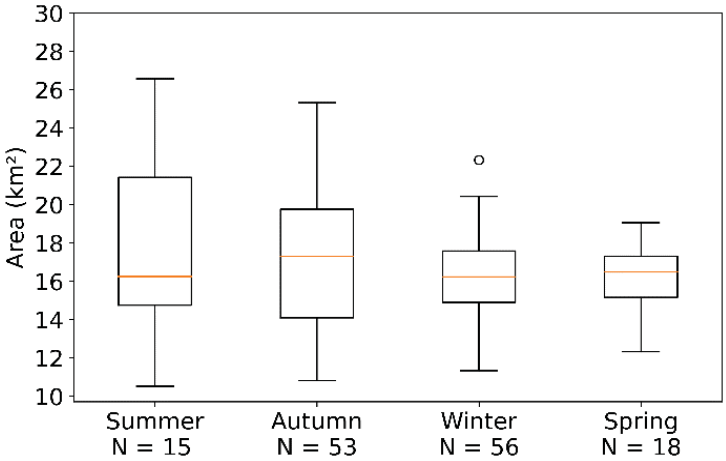

SOURCE: The Author (2022).

Moreover, aiming at a trend analysis of extreme values, the permanence curve was also calculated for the maximum area recorded in each year (FIGURE 21). The curve followed a decreasing linear behavior and was fitted to a 1st degree polynomial ($R^2 = 0.94$). Although the coefficient of determination is high, by the linear adjustment, the low frequency values (0% -10%, range that, for this analysis, is considered the most worrying) are underestimated when observed in the historical series. However, for the other frequencies, the adjustment was satisfactory. For most of the time (frequencies > 50%) the maximum area values ranged from 12 to 18 km², while for areas with higher macrophyte occupancy, that is, frequencies between 0 and 10%, there was a jump of 6 km².

As there is periodicity between the data in this series, the time of occurrence associated with the macrophytes permanence was also calculated (FIGURE 22). The data follow a similar behavior to a logarithmic growth and were also adjusted (R^2 = 0.92). In this case, despite the coefficient of determination being high and well representative by the logarithmic adjustment for almost the entire series, the value associated with the longest time interval (35 years, a value that, for this analysis, is considered the most worrying) was overestimated.

Once more, in both analyses, it was found that the areas with the highest values correspond to the most recent decades, while the smaller areas correspond to the 1980s.

FIGURE 21 - PERMANENCE CURVE OF MAXIMUM MACROPHYTE AREAS AND ITS RESPECTIVE LINEAR ADJUSTMENT.

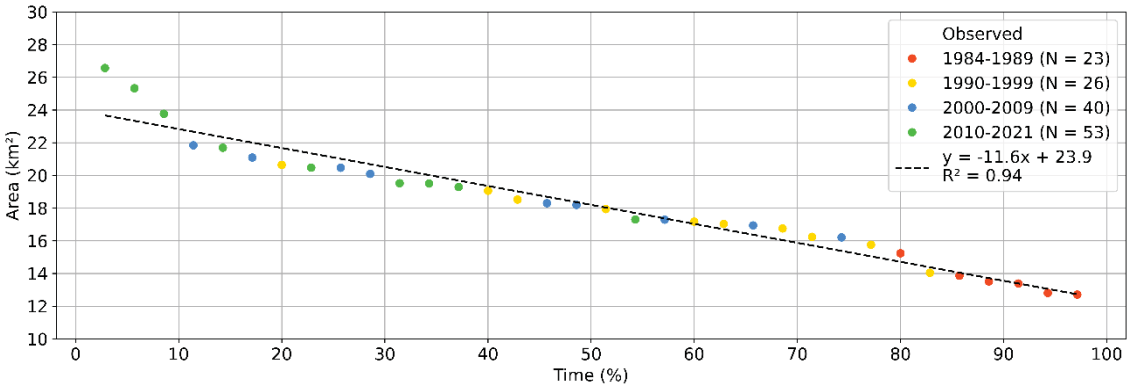

SOURCE: The Author (2022).

FIGURE 22 - RETURN TIME CURVE OF MAXIMUM MACROPHYTE AREAS AND ITS RESPECTIVE LOGARITHMIC FIT.

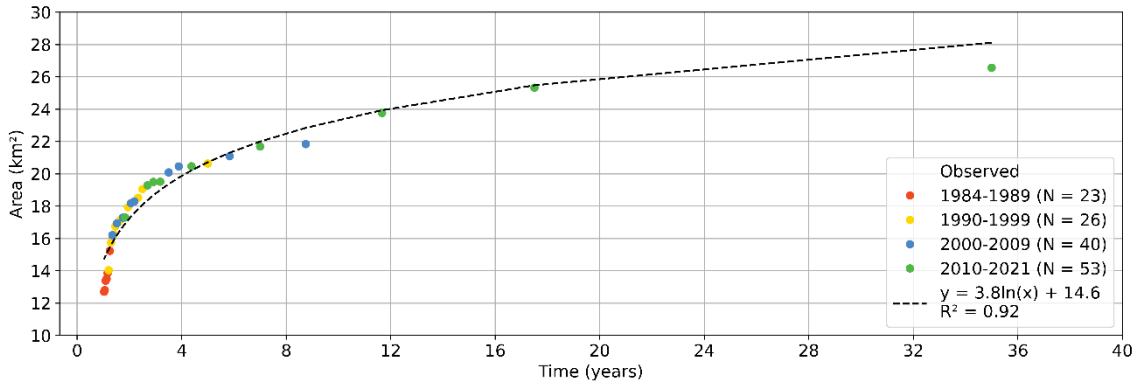

SOURCE: The Author (2022).

4.4 MACROPHYTE AREA PERMANENCE MAPS

Even before it is possible to calculate the area, the identification of macrophytes in the images through the application of the macrophyte mask using the GSAVI index (0.024-0.294) provides the spatial distribution in the reservoir, which made it possible to calculate the spatial shape permanence. For better visualization, the spatial distribution of macrophyte permanence was divided into three classes: low permanence (in blue), intermediate permanence (in green) and high permanence (in red) (FIGURE 23).

In the entire reservoir, three regions are worth mentioning. The first one is a stretch of the Tietê River, where, even with low permanence values, at some point almost all its extension was already occupied by macrophytes. Besides this low permanence, these values represent more recent areas of occupation, which indicates that macrophytes are developing in new areas of the reservoir. Another highlighted region is the initial stretch of the Paraná River, where we can observe the presence of macrophytes with greater permanence near the bank, while more central regions present lower permanence. As for the initial stretch of the Sucuriú River, it stands out for the high number of regions with a high permanence of macrophytes. For the other areas, in general, there is a predominance of macrophytes at the reservoir banks (FIGURE 23).

For each of these three regions, the permanence was mapped considering seasonal variations and variations over the decades (FIGURE 24, FIGURE 25 and FIGURE 26).

In the Tietê River, it is noted from Spring to Summer there is an increase in the occupied area and permanence, while from Summer to Autumn there is an increase in area and a decrease in permanence. From Autumn to Winter, there is a decrease in both area and permanence, while from Winter to Spring there is a reduction in area, but an increase in permanence. These last two behaviors were also observed in a branch of the Itaipu reservoir, located about 550 km downstream from Jupiá (Rosa et al., 2018). It is also noteworthy there are regions in left bank which present intermediate permanence throughout all seasons, which may indicate regions of active renewal of these organisms (such as macrophyte nurseries) (FIGURE 24).

FIGURE 23 - MACROPHYTE PERMANENCE MAP FOR THE ENTIRE PERIOD 1984-2021* (*EXCEPT FOR THE YEARS: 2003, 2011, 2012 AND 2013).

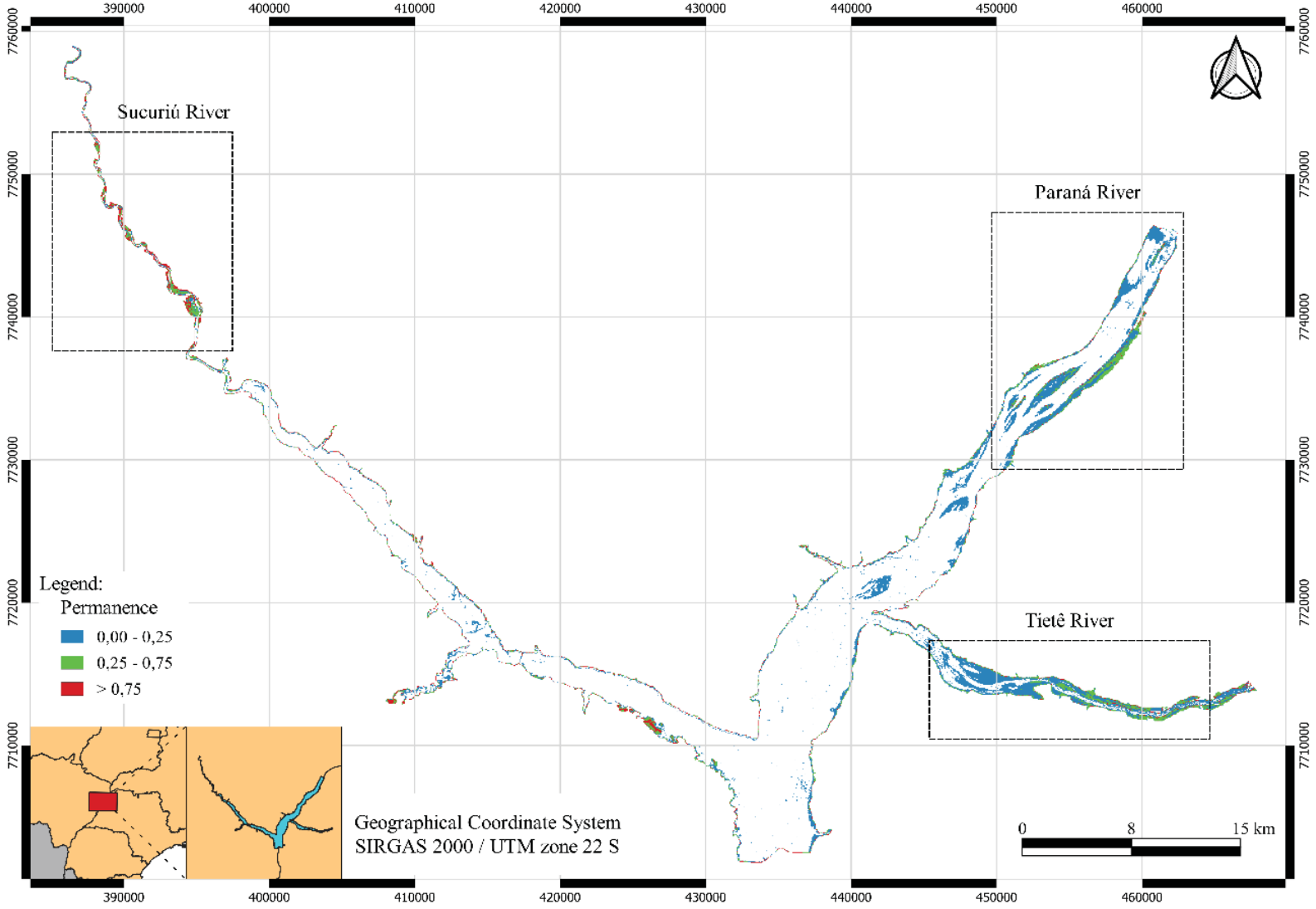

SOURCE: The Author (2022).

FIGURE 24 - PERMANENCE MAP DETAILING FOR THE TIETÊ RIVER REGION WITH VARIATIONS BETWEEN SEASONS AND DECADES.

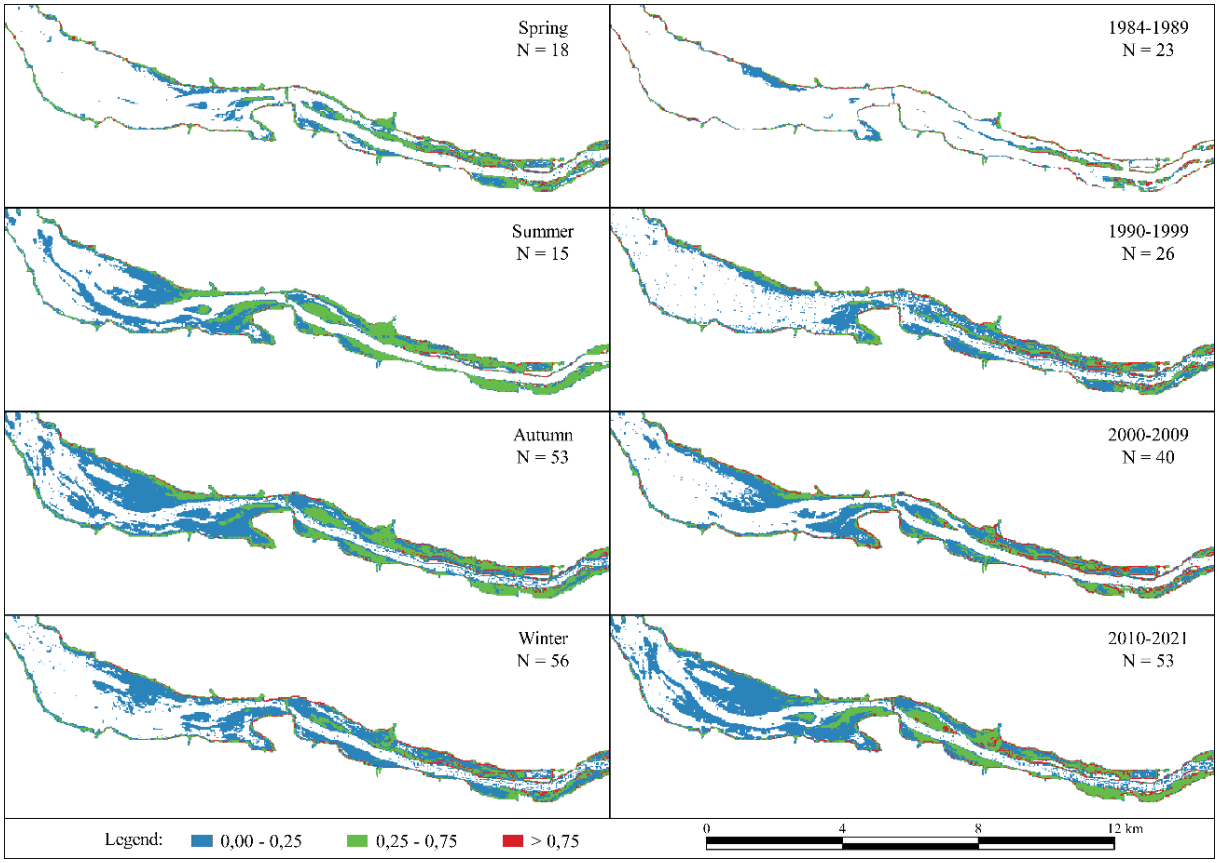

SOURCE: The Author (2022).

Likewise, for the variation between decades, the general behavior over the years was an increase in occupied area and permanence. In the 1980s there was a predominance of macrophytes on the banks reaching high permanence values, while from the 1990s the area extends to the center of the channel. Subsequently, in the 2000s, there was a clearer delimitation of macrophyte areas (such as island formations in the channel center) and an increase in permanence in regions close to the banks. This behavior became even more pronounced in the 2010s (FIGURE 24) and is associated with lower flow velocities that, due to the channel geometry, end up becoming shelters for the development and establishment of these organisms (THOMAZ, 2002). This result corroborates another study wherein it was found that the 53% increase in the area of macrophytes in the São Francisco River was observed on the bank with lower speed and depth, rather than on the bank where there is navigation (MINHONI et al., 2018).

Conversely, for the Paraná River (FIGURE 25), mainly in the region of Ferradura island and for the left bank (considering the river flow direction), from Spring

to Summer there is an increase in the area of occupation and a decrease in permanence, while from Summer to Autumn there is a decrease in the area of occupancy and increased permanence. This behavior is repeated from Autumn to Winter and from Winter to Spring (FIGURE 25). Variations in area and permanence over the decades occurred similarly to the Tietê River, with emphasis on the increase in area on the left bank and on Ferradura island.

Otherwise, in the Sucuriú River the variation is not as pronounced as in the other analyzed regions, both for the variation between seasons and over the decades. Here it is noted that the Summer was the season that presented shorter permanence than others, and in the Spring, there were more areas with high permanence. As for the permanence variation over the decades, despite the areas remaining constant, it is noted the 1990s presented higher permanence for the areas occupied by macrophytes and that this value decreased over the following years, with the 2010s permanence lower than 2000s (FIGURE 26).

FIGURE 25 - PERMANENCE MAP DETAILING FOR THE PARANÁ RIVER REGION WITH VARIATIONS BETWEEN SEASONS AND DECADES.

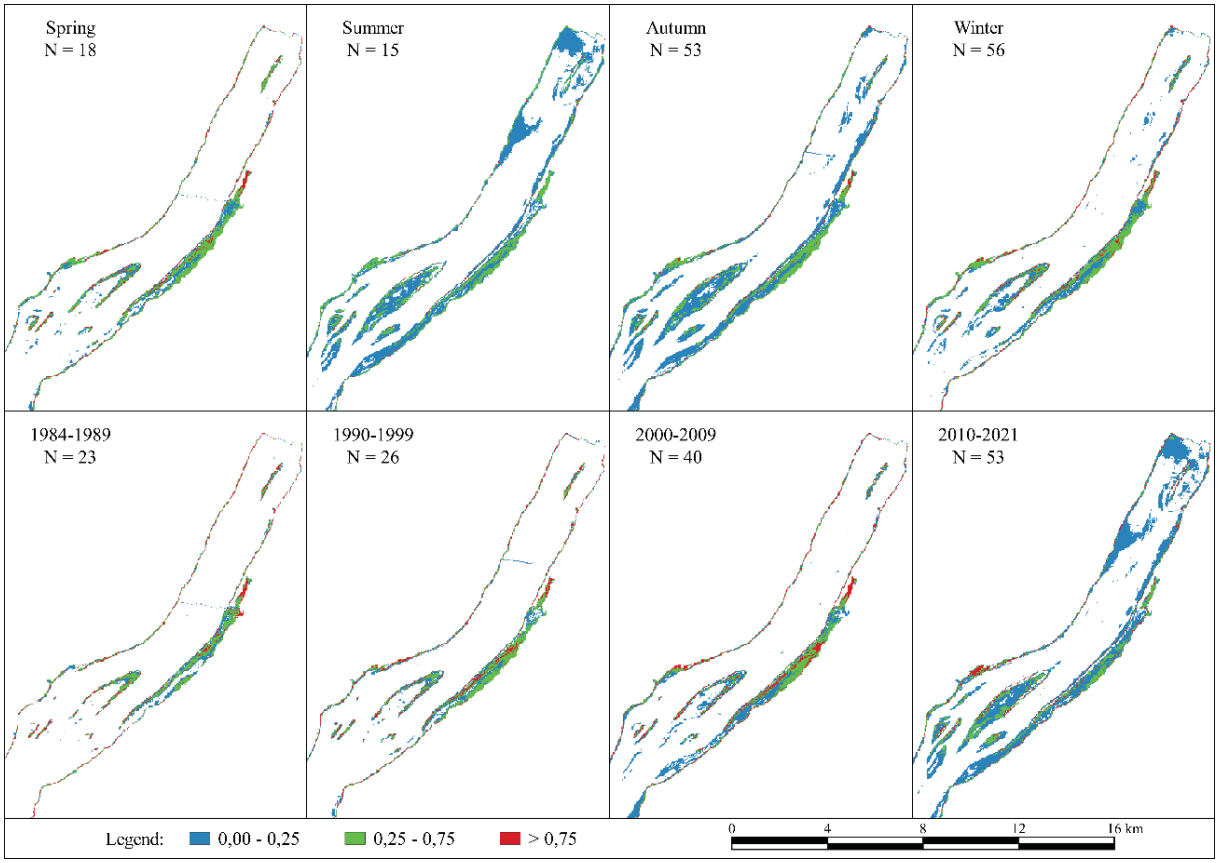

SOURCE: The Author (2022).

FIGURE 26 - PERMANENCE MAP DETAILING FOR THE SUCURIÚ RIVER REGION WITH VARIATIONS BETWEEN SEASONS AND DECADES.

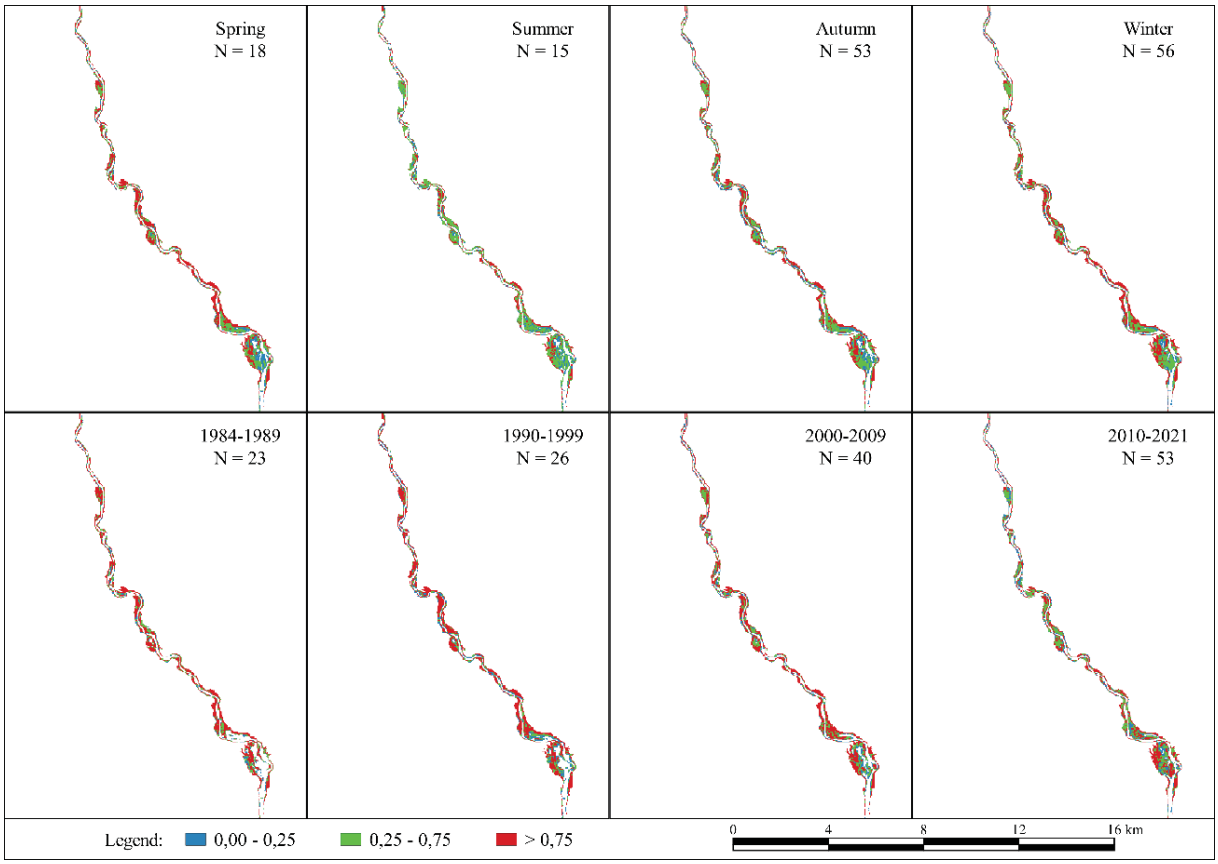

SOURCE: The Author (2022).

4.5 ENVIRONMENTAL VARIABLES EFFECTS ON MACROPHYTE GROWTH

After verifying macrophyte area growth trends over time and seasonal variations, some limiting factors to macrophyte growth were analyzed in order to verify if and which environmental variable contributed to these processes.

4.5.1 Land use analysis

For the four basins analyzed (Jupiá basin, and the incremental basins of the Ilha Solteira and Três Irmãos HPP and the Sucuriú River), in general, it was verified a decrease in natural areas of forest and non-forest natural formations (eg. fields and rock formations) while increasing the coverage of agricultural activities and non-vegetated areas (eg. urban areas and mining) (FIGURE 27).

The incremental basin of the Sucuriú River (with the smallest area) was the one that presented the greatest variation in land use; however, this variation is small when compared to the basin total area (Jupiá). This fact may indicate the presence of agricultural activities in this region is contributing to the high permanence of macrophytes in this reservoir area.

Macrophyte growth was also associated with nutrient concentration in the Paraíba do Sul River (São Paulo, Brazil) (LIMA et al., 2018), but due to population growth and, consequently, to environmental problems caused by it, such as incorrect disposal waste. Meanwhile, Minhoni et al. (2017) raised as a possible reason for 50% macrophytes area increase in Barra Bonita reservoir between 2014 and 2015, the decrease in the reservoir discharge (due to less precipitation in the period). The authors also noticed greater macrophytes agglomeration in places with less water volume and associated this with a greater nutrient's concentration.

FIGURE 27 - LAND USES VARIATION IN THE JUPIÁ WATERSHED AND IN THE INCREMENTAL WATERSHEDS (ILHA SOLTEIRA, TRÊS IRMÃOS AND SUCURIÚ) BETWEEN 1985 AND 2020.

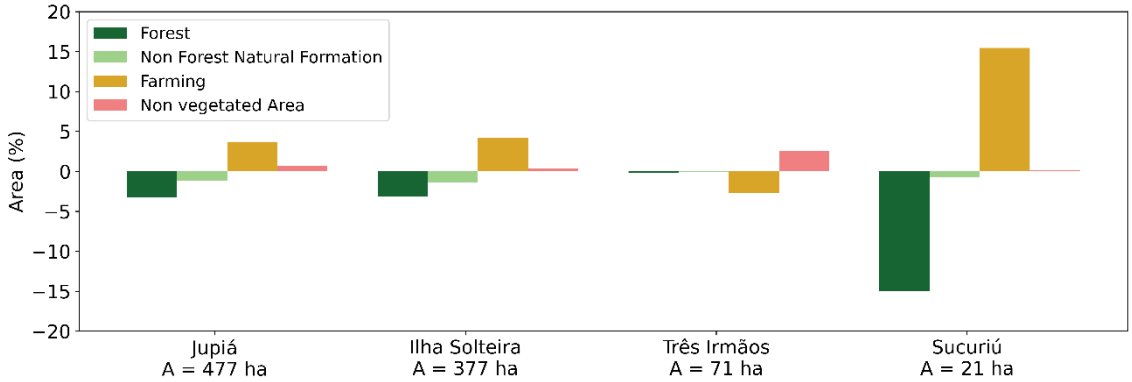

SOURCE: The Author (2022).

4.5.2 Temperature and precipitation analysis

Although Jupiá reservoir is in a tropical region, the macrophyte area showed similar behavior to macrophyte species from temperate climates over the last 8 years (FIGURE 28). In general, primary productivity reaches the highest rates during Spring, when shoots appear and, as temperature and solar radiation increase, leaves also develop. During the Summer, productivity is lower than in the previous season, however it's when the highest biomass values are recorded. At the end of this season,

the formation of debris begins, and by the end of Autumn the community is practically dead (ESTEVES, 1998).

This cyclical and seasonal behavior coincides with what was observed in climatological variables such as precipitation and temperature, since the availability of light impacts photosynthetic processes and higher temperatures act as catalysts. However, Luo et al. (2016) found that the growth of certain macrophyte species responds faster to temperature than others, so that the cyclic behavior may be time-shifted.

FIGURE 28 - SEASONAL VARIATION OF MONTHLY PRECIPITATION, MONTHLY MEAN TEMPERATURE AND MACROPHYTE AREA OVER 2014-2021.

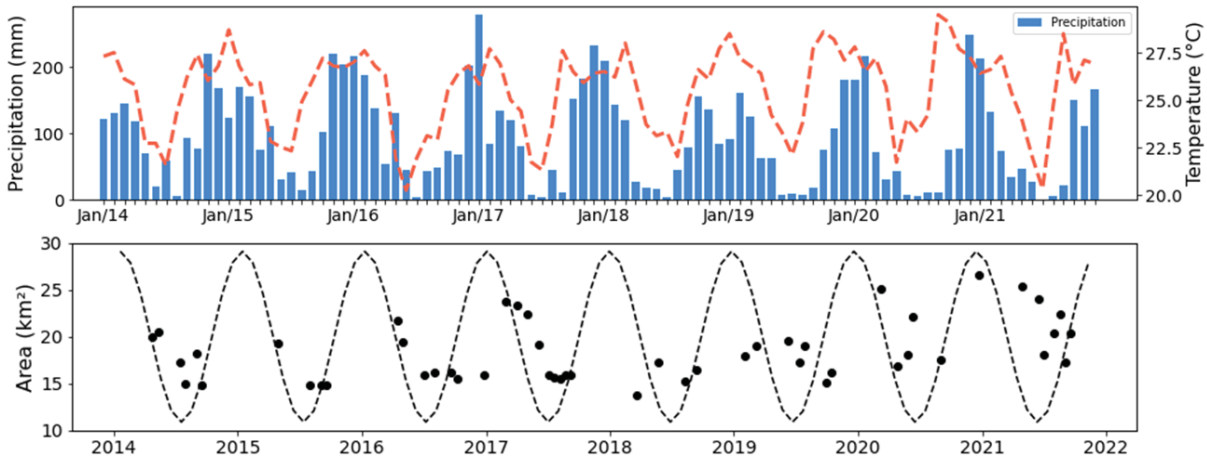

SOURCE: The Author (2022).

4.5.3 Upstream HPP discharge analysis

When comparing the macrophyte area data with the operational discharge of the plants upstream Jupiá reservoir, it is worth highlight the first macrophyte area peak (October/1991) follows the filling (CESTARI JUNIOR; CELERI, 1999) and the beginning of the spill (April/1991) of the Três Irmãos reservoir (FIGURE 29). The interval between these events could be justified by the fact that spill started in a period when naturally there is senescence of these organisms (Autumn) and the macrophyte peak occurs in the season when primary production reaches the highest rates (Spring), as described above.

Likewise, the formation of the Três Irmãos reservoir may have contributed to the increase in the amount of nutrients in the water, due to the biomass decomposition

process inside the reservoir, while the Tietê River damming may have caused the decrease of the downstream current velocity, providing a peaceful and more favorable environment for macrophytes development.

Furthermore, in April/1991 there was also a peak of maximum monthly flows spillway and outflow at Ilha Solteira HPP, and the hourly value recorded ($Q_{out\ max}$ = 23,526 m³/s e $Q_{spill\ max}$ = 17,000 m³/s) was the highest of all the historic serie.

FIGURE 29 - MAXIMUM MONTHLY (HOURLY) OUTFLOW, SPILLWAY AND TURBINE DISCHARGE AT ILHA SOLTEIRA AND TRÊS IRMÃOS HPP.

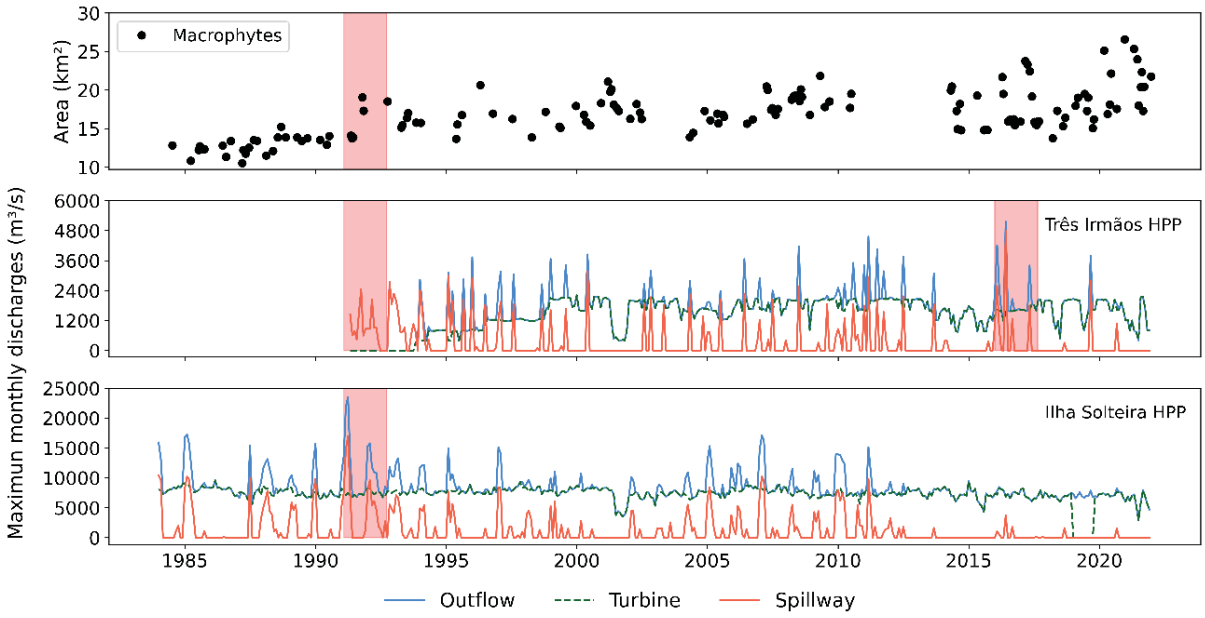

SOURCE: The Author (2022).

When it is analyzed the flows from Três Irmãos HPP, there was a peak of maximum monthly flows spillway and outflow in June/2016, with the recorded hourly value ($Q_{out\ max}$ = 5,160 m³/s and $Q_{spill\ max}$ = 4,795 m³/s) was the highest of the entire historical series. When it is analyzed the 2017 event, although there was also a peak, the monthly maximum hourly flows ($Q_{out\ max}$ = 3,401 m³/s and $Q_{spill\ max}$ = 1,799 m³/s) were lower than those recorded in 2016. Although the effluent volume in 2017 was 23.7% lower than in 2016, in the 2017 event there were consecutive abrupt increases in discharge, the first being at the beginning of the event (1,167 m³/s in 4h), followed by another 16h later (1,828 m³/s in 11h) in addition to 2 cycles of decrease and increase (1,209 m³/s in 2 and 3h, 961m³/s in 2h and 1,209m³/s in 4h) 39h after the start of the event (FIGURE 30).

However, when we consider the inputs through the Paraná River, despite a slight increase in spillway discharge in 2016, in 2017 the outflow discharge remained at the same magnitude (FIGURE 29).

FIGURE 30 - COMPARISON BETWEEN JUNE/2016 AND MAY/2017 OPERATIONS IN TRÊS IRMÃOS HPP.

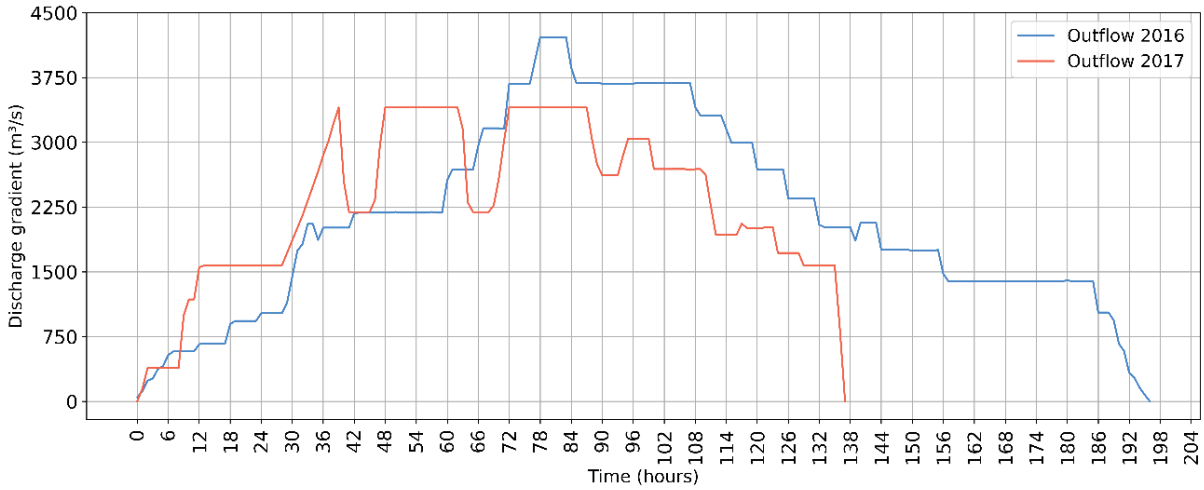

SOURCE: The Author (2022).

Considering that: (i) the mapped area close to the date of these two events is similar; (ii) that in terms of total area, they did not stand out throughout the historical series and; (iii) both events happen in Autumn; it is may be possible that the reason why, unlike in 2016, the 2017 event caused impacts both on the spatial arrangement of macrophytes (FIGURE 13 and FIGURE 14) on energy generation could be related to the outflow discharge to Jupiá reservoir.

5 FINAL CONSIDERATIONS

In summary, the use of the GEE platform enabled the use of a significant number of images quickly, free of charge and without the need of computers with high processing power. Despite the amount of satellite images being a limitation, due to interferences such as sunlight or cloud cover, satellite images used to set up a historical series of macrophyte occupation in the Jupiá reservoir proved to be very satisfactory. This study can be widely expanded to other reservoirs, since nowadays there is still a lack of historical information about their evolution, despite the monitoring of these organisms being a current concern (given the damage caused to energy generation, for example).

The knowledge of the total area and the spatial arrangement of macrophytes over the years allowed us to observe, besides the growth trend, cyclical behaviors coinciding with interannual climatic seasonality, such as detachment and/or death trends of organisms between two consecutive seasons. This information can and should be used as a basis for decision-making regarding monitoring, removal and management of these organisms, thus contributing to ensuring the multiple uses of water.

Another factor to be highlighted is that the outflow discharge on may have caused the displacement of a significant amount of macrophytes from the Tietê River to the Jupiá dam in 2017, causing the interruption of energy generation. Even though the macrophyte mapped area in this event is high, it was not the largest recorded in the entire series. The realization of this fact raises an alert that, as there is a tendency for macrophyte areas to grow (regardless of the interannual variations verified), if in the future there is a need for a similar operation, the severity of the impacts on energy generation also tends to be greater than recorded in 2017.

Although some limiting factors to the growth of macrophytes have been verified, due to the complexity of the interaction of macrophytes with the environment, the use of satellite images to analyze the temporal evolution of physicochemical variables is suggested as a topic for future research, to verify other reasons for the increase in the coverage of macrophytes, especially after the construction of the Três Irmãos reservoir.

ACKNOWLEDGEMENTS

The authors would like to thank the Instituto de Tecnologia para o Desenvolvimento (LACTEC) and China Three Gorges Brasil (CTG Brasil) for providing data and for funding this research trough P&D ANEEL n° 10381- 0819/2019 (Plano de Ações Emergenciais para Macrófitas, em reservatórios hidroelétricos, resultante de monitoramento inteligente do crescimento e deslocamento em tempo real). Tobias Bleninger acknowledges the productivity stipend from the National Council for Scientific and Technological Development – CNPq, grant no. 312211/2020-1, call no. 09/2020.

REFERENCES

ANEEL – AGÊNCIA NACIONAL DE ENERGIA ELÉTRICA **Banco de Informação de Geração**. 2019. Disponível em: http://www2.aneel.gov.br/aplicacoes/capacidadebrasil/capacidadebrasil.cfm.

ASAEDA, T.; TRUNG, V. K.; MANATUNGE, J. Modelling macrophyte-nutrient-phytoplankton interactions in shallow eutrophic lakes and the evaluation of environmental impacts. **Ecological Engineering**, v. 16, n. 3, p. 341–357, 2000. Disponível em: https://doi.org/10.1016/S0925-8574(00)00120-8.

BAI, G.; ZHANG, Y.; YAN, P.; YAN, W.; KONG, L.; WANG, L.; WANG, C.; LIU, Z.; LIU, B.; MA, J.; ZUO, J.; LI, J.; BAO, J.; XIA, S.; ZHOU, Q.; XU, D.; HE, F.; WU, Z. Spatial and seasonal variation of water parameters, sediment properties, and submerged macrophytes after ecological restoration in a long-term (6 year) study in Hangzhou west lake in China: Submerged macrophyte distribution influenced by environmental variables. **Water Research**, v. 186, 2020. Disponível em: https://doi.org/10.1016/j.watres.2020.116379.

BEZERRA JUNIOR, A. Monitoramento de macrófitas aquáticas no reservatório 25 de março, município de Pau dos Ferros, oeste potiguar (RN/BR). **Geofronter**, 7, 1–15, 2021.

BIANCHINI JUNIOR., I. Modelos de crescimento e decomposição de macrófitas aquáticas. In Thomaz, T. S. & Bini, L. M. (Eds.), **Ecologia e Manejo de Macrófitas**. Maringá: Editora da Universidade Estadual de Maringá, 2003.

BIUDES, J. F. V.; CAMARGO, A. F. M. Estudo dos fatores limitantes à produção primária por macrófitas aquáticas no Brasil. **Oecologia Australis**, v. 12, n. 01, p. 7–19, 2008. Disponível em: https://doi.org/10.4257/oeco.2008.1201.01.

BOSCHI, L. S.; GALO, M. L. B. T.; ROTTA, L. H. S.; WATANABE, F. S. Y. Mapeamento do biovolume de plantas aquáticas submersas a partir de dados

hidroacústicos e imagem multiespectral de alta resolução. **Planta Daninha**, v. 30, n. 3, p. 525–539, 2012. Disponível em: https://doi.org/10.1590/S0100-83582012000300008.

BRASIL. Empresa de Pesquisa Energética. **Balanço Energético Nacional 2021: Ano base 2020** / Rio de Janeiro: EPE, 2021.

BRIX, H.; SCHIERUP, H.H. The use of aquatic macrophytes in water. **Pollution control Ambio**.v.15, p. 100-107, 1989.

CAMARGO, A. F. M.; PEZZATO, M. M.; HENRY-SILVA, G. G. Fatores limitantes à produção primária de macrófitas aquáticas características. In: THOMAZ, S. M.; BINI, L. M. (Eds.). **Ecologia e manejo de marófitas**. Maringá: Editora da Universidade Estadual de Maringá Reitor:, 2003.

CANCIAN, L. F.; CAMARGO, A. F. M.; SILVA, G. H. G. Crescimento das macrófitas aquáticas flutuantes Pistia stratiotes e Salvinia molesta em diferentes condições de temperatura e fotoperíodo. **Acta Botanica Brasilica**, v. 23, n. 2, p. 552–557, 2009. Disponível em: https://doi.org/10.1590/S0102-33062009000200027.

CESTARI JUNIOR., E.; CELERI, A. Reflexos do enchimento do reservatório da UHE Três Irmãos nas edificações da cidade de Pereira Barreto. In: **Anais do Seminário Nacional de Grandes Barragens**, Belo Horizonte. v. 2, p. 79- 86, 1999.

CHEN, F.; ZHANG, M.; TIAN, B.; LI, Z. Extraction of Glacial Lake Outlines in Tibet Plateau Using Landsat 8 Imagery and Google Earth Engine. **IEEE Journal of Selected Topics in Applied Earth Observations and Remote Sensing**, v. 10, n. 9, p. 4002–4009, 2017. Disponível em: https://doi.org/10.1109/JSTARS.2017.2705718.

CHINA THREE GORGES BRASIL ENERGIA LTDA (CTG Brasil). **CTG Brasil website**. 2019. Não paginado. Disponível em: https://www.ctgbr.com.br/ctg-brasil-investe-r-46-milhoes-em-projeto-para-transformar-plantas-aquaticas-em-biocombustivel/. Acesso em: 28 out. 2021

CHINA THREE GORGES BRASIL ENERGIA LTDA (CTG Brasil). **Sistema de Monitoramento de Macrófitas**. Não paginado. Disponível em: https://ctgbr.eastus.cloudapp.azure.com/portal/apps/Cascade/index.html?appid=a942754c2ebf41c88cbc50d3a3a39ef7. Acesso em 13 dez.2021.

CHINA THREE GORGES BRASIL ENERGIA LTDA (CTG Brasil). **vazoes_ctg.csv** 51.798 Kb. Formato CSV. Curitiba, 2022.

CLIMATE HAZARDS GROUP INFRARED PRECIPITATION WITH STATION DATA (CHIRPS). 2022. Disponível em: https://developers.google.com/earth-engine/datasets/catalog/UCSB-CHG_CHIRPS_DAILY.

COLADELLO, L. F.; GALO, M. L. B. T.; SHIMABUKURO, M. H.; IVÁNOVÁ, I.; AWANGE, J. Macrophytes' abundance changes in eutrophicated tropical reservoirs exemplified by Salto Grande (Brazil): Trends and temporal analysis exploiting Landsat

remotely sensed data. **Applied Geography**, 121, 2020. Disponível em: https://doi.org/10.1016/j.apgeog.2020.102242.

CORDEIRO, A. P. A.; BERLATO, M. A.; FONTANA, D. C.; MELO, R. W. de; SHIMABUKURO, Y. E.; FIOR, C. S. Regiões homogêneas de vegetação utilizando a variabilidade do NDVI. **Ciência Florestal**, v. 27, n. 3, p. 883–896, 2017. Disponível em: https://doi.org/10.5902/1980509828638.

CUNHA-SANTINO, M. B.; BIANCHINI JUNIOR, I. Modelos matemáticos aplicados aos estudos de decomposição de macrófitas aquáticas. **Oecologia Brasiliensis**, v. 10, n. 02, p. 154–164, 2006. Disponível em: https://doi.org/10.4257/oeco.2006.1002.03.

DEZORDI, R.; KRAMER, G.; NIEDERAURER, C.; DAL, J. Análise da turbidez superficial a partir de imagens do Landsat-8 (Sensor OLI) em compartimento aquático do reservatório de Itaipu-PR, Brasil. **Anais do XIX Simpósio brasileiro de Sensoriamento Remoto**. v. 8, p. 2953–2955, Santos, 2015.

ESTEVES, F. de A. **Fundamentos de Limnologia.** Rio de Janeiro: Interciencia. 1998.

FANG, Y.; LI, H.; WAN, W.; et al. Assessment of water storage change in China's lakes and reservoirs over the last three decades. **Remote Sensing**, v. 11, n. 12, 2019. Disponível em: https://doi.org/10.3390/rs11121467

FREITAS, A. de; SIDINEI, M. T. Inorganic carbon shortage may limit the development of submersed macrophytes in habitats of the Paraná River basin. **Acta Limnologica Brasiliensia**, v. 23, n. 1, p. 57–62, 2011. Disponível em: https://doi.org/10.4322/actalb.2011.019

GALO, M. L. B. T. VELINI, E.D.; TRINDADE, M.L.B.; SANTOS, S.C.A.. Uso do sensoriamento remoto orbital no monitoramento da dispersão de macrófitas nos reservatórios do complexo Tietê. **Planta Daninha**, v. 20, n. spe, p. 7–20, 2002. Disponível em: https://doi.org/10.1590/S0100-83582002000400002.

GIMENES, L. L. S.; FRESCHI, G. P. G.; BIANCHINI JÚNIOR, I.; SANTINO, M. B. C. Growth of the aquatic macrophyte Ricciocarpos natans (L.) Corda in different temperatures and in distinct concentrations of aluminum and manganese. **Aquatic Toxicology**, v. 224, n. April, p. 8, 2020. Disponível em: https://doi.org/10.1016/j.aquatox.2020.105484.

GITELSON, A. A., KAUFMAN, Y. J., & MERZLYAK, M. N. Use of a green channel in remote sensing of global vegetation from EOS-MODIS. **Remote Sensing of Environment**, 58(3), 289–298, 1996. Disponível em: https://doi.org/10.1016/S0034-4257(96)00072-7.

GIUSTI, E.; MARSILI-LIBELLI, S. Modelling the interactions between nutrients and the submersed vegetation in the Orbetello Lagoon. **Ecological Modelling**, v. 184, n. 1, p. 141–161, 2005. Disponível em: https://doi.org/10.1016/j.ecolmodel.2004.11.014.

Google Earth Engine. 2022. Recuperado de: http:// https://code.earthengine.google.com.

HUETE, A. R. A Soil-Adjusted Vegetation Index (SAVI). **Remote Sensing of Environment**, 25(3), 295–309, 1988. Disponível em: https://doi.org/10.1016/0034-4257(88)90106-X.

Instituto de Tecnologia para o Desenvolvimento – LACTEC. **Relatório Técnico Final, Etapa 3: Integração com sistema de monitoramento hidrológicos, Atividade 3 Modelagem de qualidade da água**, Curitiba, 2019a. Relatório técnico.

Instituto de Tecnologia para o Desenvolvimento - LACTEC. **Relatório Técnico Final, Etapa 2: Desenvolvimento de algoritmo para identificação de macrófitas, Atividade 2: Campanhas de campo para qualidade da água e macrófitas, Volume I – Levantamento Florístico e de Biomassa Fresca e Qualidade da Água e Sedimentos**. Curitiba, 2019b. Relatório técnico.

Instituto de Tecnologia para o Desenvolvimento - LACTEC. **Relatório Técnico Final, Etapa 4: Integração com GIS corporativo em ArcGIS Portal, Atividade 1: Desenvolvimento do módulo de Alertas**. Curitiba, 2019c. Relatório técnico.

Instituto de Tecnologia para o Desenvolvimento - LACTEC. **Relatório Técnico Final**, **Etapa 2: Desenvolvimento de algoritmo para identificação de macrófitas, Atividade 2: Campanhas de campo para qualidade da água e macrófitas, Volume II – Levantamentos Batimétricos e Aerolevantamentos com VANT**, Curitiba, 2019d. Relatório técnico.

Instituto de Tecnologia para o Desenvolvimento - LACTEC. **Relatório Técnico Final, Etapa 1- Instrumentação do Reservatório com Enfoque no Monitoramento em Tempo Real de Macrófitas, Atividade 1: Definição dos locais críticos para estudo**. Curitiba, 2020. Relatório técnico.

JAVED, T.; YAO, N.; CHEN, X.; SUON, S.; LI, Y. Drought evolution indicated by meteorological and remote-sensing drought indices under different land cover types in China. **Environmental Science and Pollution Research**, v. 27, n. 4, p. 4258–4274, 2020. Disponível em: https://doi.org/10.1007/s11356-019-06629-2.

JIANG, D.; MATSUSHITA, B.; SETIAWAN, F.; VUNDO, A. An improved algorithm for estimating the Secchi disk depth from remote sensing data based on the new underwater visibility theory. **ISPRS Journal of Photogrammetry and Remote Sensing**, v. 152, n. November 2018, p. 13–23, 2019. Disponível em: https://doi.org/10.1016/j.isprsjprs.2019.04.002.

LANDIS, J. R.; KOCH, G. G. An Application of Hierarchical Kappa-type Statistics in the Assessment of Majority Agreement among Multiple Observers. **Biometrics**, 33(2), 363–374, 1977. Disponível em: https://doi.org/10.2307/2529786.

LI, H.; LUO, Z.; XU, Y.; ZHU, S.; CHEN, X.; GENG, X.; XIAO, L.; WAN, W.; CUI, Y. A remote sensing-based area dataset for approximately 40 years that reveals the hydrological asynchrony of Lake Chad based on Google Earth Engine. **Journal of Hydrology**, v. 603, p. b, 126934, 2021. Disponível em: https://doi.org/10.1016/j.jhydrol.2021.126934.

LIMA, B. A. de A.; LIBÓRIO, M. P.; HADAD, R. M. Análise espaço-temporal do crescimento de macrófitas e sua aplicação no monitoramento da qualidade da água. **RAEGA,** v. 45, n. 1, p. 45–57, 2018. Disponível em: https://doi.org/10.5380/raega.

LIMA, D. R. M. de.; DLUGOSZ, F. L.; IURK, M. C.; PESCK, V. A. Uso de NDVI e SAVI para caracterização da cobertura da Terra e análise temporal em imagens RapidEye. **Revista Espacios**, v. 38, 2017.

LOBO, F. de L.; NAGEL, G. W.; MACIEL, D. A.; CARVALHO, L. A. S. de.; MARTINS, V. S.; BARBOSA, C. C. F.; NOVO, E. M. L. de M. Algaemap: Algae bloom monitoring application for inland waters in Latin America. **Remote Sensing**, v. 13, n. 15, 2021. Disponível em: https://doi.org/10.3390/rs13152874.

LUO, J.; LI, X.; MA, R.; LI, F.; DUAN, H.; HU, W.; QIN, B.; HUANG, W. Applying remote sensing techniques to monitoring seasonal and interannual changes of aquatic vegetation in Taihu Lake, China. **Ecological Indicators**, 60, 503–513, 2016. Disponível em: https://doi.org/10.1016/j.ecolind.2015.07.029.

MACHADO, R. **Efeitos da temperatura e da turbidez no crescimento de Egeria densa Planch**. 2020. 113f. Tese (Doutorado em Ecologia e Recursos Naturais) – Centro de Ciências Biológicas e da Saúde, Universidade Federal de São Carlos, São Carlos, 2020.

MARTINE, J. M.; SEYLER, F.; BOURGOIN, L. M.; MOREIRA-TURCQ, P.; GUYOT, J. L. Amazon basin water quality monitoring using MERIS and MODIS data**. European Space Agency,** Special Publication , n. 572, p. 1697–1706, 2005.

MENDES, W. DE S.; DEMATTÊ, J. A. M.; DE RESENDE, M. E. B.; et al. A remote sensing framework to map potential toxic elements in agricultural soils in the humid tropics. **Environmental Pollution**, v. 292, n. July 2021, 2022. Disponível em: https://doi.org/10.1016/j.envpol.2021.118397

MESQUITA, F. de O.; ALVES, A. DE S.; MALHEIROS, S. M. M.; SILVA, P. C. M. da.; SANTOS, W. de O.; BATISTA, R. O.Uso do sensoriamento remoto para avaliação da distribuição espacial e quantificação de Macrófitas na barragem Umari – Upanema, RN. **Agropecuária Científica no Semiárido**, v. 9, n. 2, p. 102–109, 2013.

MINHONI, R. T. de A., SOUZA, M. H. C. de, SANTOS, R. D. da S., ZIMBACK, C. R. L. Monitoramento de macrófitas aquáticas no rio São Francisco no trecho urbano de Petrolina-PE. **Scientia Plena**, 14(3), 1–9, 2018. Disponível em: https://doi.org/10.14808/sci.plena.2018.039901.

MINHONI, R. T. de A.; PINHEIRO, M. P. M. A.; FILGUEIRAS, R.; ZIMBACK, C. R. L. Sensoriamento remoto aplicado ao monitoramento de macrófitas aquáticas no reservatório de barra Bonita, SP. **Irriga**, 22(2), 330–342, 2017. Disponível em: https://doi.org/10.15809/irriga.2017v22n2p330-342.

MUSTAFA, A. L., DIAS, J. H. P., BONAFÉ, R. de A., & BELMONT, R. A. F. A Experiência Da CESP No Manejo e Controle de Macrófitas No Reservatório Da UHE Engenheiro Souza Dias (Jupiá). **Ação Ambiental,** 44, 17–26, 2010.

MUTANGA, O.; KUMAR, L. Google earth engine applications. **Remote Sensing**, v. 11, n. 5, p. 11–14, 2019. Disponível em: https://doi.org/10.3390/rs11050591.

NAGHETTINI, M.; PINTO, E. J. A. **Hidrologia Estatística**. Belo Horizonte: CPRM, 2007.

Novo, E. M. L. M. **Sensoriamento remoto: princípios e aplicações**. São Paulo: Edgard Blücher, 1998.

OYAMA, Y.; MATSUSHITA, B.; FUKUSHIMA, T. Distinguishing surface cyanobacterial blooms and aquatic macrophytes using Landsat/TM and ETM+ shortwave infrared bands. **Remote Sensing of Environment**, v. 157, p. 35–47, 2015. Disponível em: https://doi.org/10.1016/j.rse.2014.04.031.

PAN, F.; XIE, J.; LIN, J.; ZHAO, T.; JI, Y.; HU, Q.; PAN, X.; WANG, C.; XI, X. Evaluation of climate change impacts on wetland vegetation in the Dunhuang Yangguan National Nature Reserve in northwest China using landsat derived NDVI. **Remote Sensing**, v. 10, n. 5, 2018. Disponível em: https://doi.org/10.3390/rs10050735.

PHILIPSON, P.; KRATZER, S.; BEN MUSTAPHA, S.; STRÖMBECK, N.; STELZER, K. Satellite-based water quality monitoring in Lake Vänern, Sweden. **International Journal of Remote Sensing**, v. 37, n. 16, p. 3938–3960, 2016. Taylor & Francis. Disponível em: https://doi.org/10.1080/01431161.2016.1204480.

POMPÊO, M. **Monitoramento e manejo de macrófitas aquáticas em reservatórios tropicais brasileiros**. 1ª ed. São Paulo: Instituto de Biociências da USP, 2017.

Projeto MapBiomas. **Coleção 6 da Série Anual de Mapas de Uso e Cobertura da Terra do Brasil**. Recuperado de: https://mapbiomas.org/.

ROSA, C. N. da; TASSI, R.; PEREIRA FILHO, W.; FAVARETTO, J R.; BENEDETTI, A. C. Ocorrência de Macrófitas Aquáticas no lado Brasileiro do Reservatório de Itaipu com o Uso de Imagens Sentinel-2a. **Revista Brasileira de Cartografia**, 70(3), 1113–1134, 2018. Disponível em: https://doi.org/10.14393/rbcv70n3-45985.

ROSA, C. N. da; TASSI, R.; PICCILLI, D. G. A.; PEREIRA FILHO, W.; FAVARETTO, J R.; FONTOURA, J. R. Identificação Do Padrão De Distribuição De Macrófitas Aquáticas Emergentes No Banhado Do Taim-Rs-Brasil, Frente a Diferentes Condições Hidrológicas. **Geociências**, v. 36, n. 4, p. 771–784, 2017. Disponível em: https://doi.org/10.5016/geociencias.v36i4.12024.

ROUSE, J. W.; HAAS, R. H.; SCHELL, J. A.; DEERING, D. Monitoring vegetation systems in the great plains with ERTS. In NASA (Ed.), **Earth resources technology satellite symposium,** v. 1, pp. 309–317, 1973.

SABO BOSCHI, L.; GALO, M. L. B. T.; ROTTA, L. H. S.; WATANABE, F. S. Y. Mapeamento do Biovolume de Plantas Aquáticas Submersas a Partir de Dados Hidroacústicos e Imagem Multiespectral de Alta Resolução. **Planta Daninha**, v. 30, n. 3, p. 525–539, 2012. Disponível em: https://doi.org/10.1590/S0100-83582012000300008.

São Paulo. Companhia Energética de São Paulo - CESP. **UHE Eng. Souza Dias (Jupiá) Plano Ambiental de Conservação e Uso do Entorno de Reservatório Artificial – PACUERA**, 2009. Relatório Técnico.

SCHAEFFER, B. A.; IIAMES, J.; DWYER, J.; URQUHART, E.; SALLS, W.; ROVER, J.; SEEGERS, B. An initial validation of Landsat 5 and 7 derived surface water temperature for U.S. lakes, reservoirs, and estuaries. **International Journal of Remote Sensing**, v. 39, n. 22, p. 7789–7805, 2018. Taylor & Francis. Disponível em: https://doi.org/10.1080/01431161.2018.1471545.

SILVA, J. C. R. **Modelagem Matemática e Simulação Computacional da Influência de Poluentes e da Velocidade de Corrente na Dinâmica Populacional de Macrófitas Aquáticas**. 2015. 155f. Tese (Doutorado em MATEMÁTICA APLICADA) – Instituto de Matemática, Estatística e Computação Científica, Universidade Estadual de Campinas, Campinas, 2015.

SUR, C.; HUR, J.; KIM, K.; CHOI, W.; CHOI, M. An evaluation of satellite-based drought indices on a regional scale. **International Journal of Remote Sensing**, v. 36, n. 22, p. 5593–5612, 2015. Taylor & Francis. Disponível em: https://doi.org/10.1080/01431161.2015.1101653.

UNIVERSIDADE ESTADUAL PAULISTA (UNESP). **Dados climáticos diários - Estação Ilha Solteira**. 2022. Disponível em: http://clima.feis.unesp.br/dados_diarios.php

TAMIMINIA, H.; SALEHIA, B.; MAHDIANPARIB, M.; QUACKENBUSHA, L.; ADELIA, S.; BRISCO B. Google Earth Engine for geo-big data applications: A meta-analysis and systematic review. **ISPRS Journal of Photogrammetry and Remote Sensing**, v. 164, n. January, p. 152–170, 2020. Disponível em: https://doi.org/10.1016/j.isprsjprs.2020.04.001.

TENA, A.; VERICAT, D.; GONZALO, L. E.; BATALLA, R. J. Spatial and temporal dynamics of macrophyte cover in a large regulated river. **Journal of Environmental Management,** 202, 379–391, 2017. Disponível em: https://doi.org/10.1016/j.jenvman.2016.11.034

THOMAZ, S.M. Fatores ecológicos associados à colonização e ao desenvolvimento de macrófitas aquáticas e desafios de manejo. *Planta Daninha*, 20, 21–33, 2002. Disponível em: https://doi.org/10.1590/s0100-83582002000400003.

TUNDISI, J. G.; TUNDISI, T. M. **Limnologia**. São Paulo: Oficina de Textos, 2008.

UDDIN, K.; MATIN, M. A.; MEYER, F. J. Operational flood mapping using multi-temporal Sentinel-1 SAR images: A case study from Bangladesh. **Remote Sensing**, v. 11, n. 13, 2019. Disponível em: https://doi.org/10.3390/rs11131581.

VILLA, P.; PINARDI, M.; BOLPAGNI, R.; GILLIER, J. G.; ZINKE, P.; NEDELCUŢ, F.; BRESCIANI, M. Assessing macrophyte seasonal dynamics using dense time series of medium resolution satellite data. **Remote Sensing of Environment**, v. 216, n. June, p. 230–244, 2018. Disponível em: https://doi.org/10.1016/j.rse.2018.06.048.

WANG, C.; JIA, M.; CHEN, N.; WANG, W. Long-term surface water dynamics analysis based on landsat imagery and the Google Earth Engine Platform: A case study in the middle Yangtze River Basin. **Remote Sensing**, v. 10, n. 10, 2018. Disponível em: https://doi.org/10.3390/rs10101635.

WATANABE, F.; ALCÂNTARA, E.; RODRIGUES, T.; et al. Remote sensing of the chlorophyll-a based on OLI/Landsat-8 and MSI/Sentinel-2a (Barra Bonita Reservoir, Brazil). **Anais da Academia Brasileira de Ciencias**, v. 90, n. 2, p. 1987–2000, 2018.

WIELAND, M.; MARTINIS, S. Large-scale surface water change observed by Sentinel-2 during the 2018 drought in Germany. **International Journal of Remote Sensing**, v. 41, n. 12, p. 4740–4754, 2020. Taylor & Francis. Disponível em: https://doi.org/10.1080/01431161.2020.1723817.

WU, Y.; LI, M.; GUO, L.; ZHENG, H.; ZHANG, H. Investigating water variation of lakes in tibetan plateau using remote sensed data over the past 20 years. **IEEE Journal of Selected Topics in Applied Earth Observations and Remote Sensing**, v. 12, n. 7, p. 2557–2564, 2019. Disponível em: https://doi.org/10.1109/JSTARS.2019.2898259.

XIONG, Y.; XU, W.; LU, N.; HUANG, S.; WU, C.; WANG, L.; DAI, F. KOU, W. Assessment of spatial–temporal changes of ecological environment quality based on RSEI and GEE: A case study in Erhai Lake Basin, Yunnan province, China. **Ecological Indicators**, v. 125, p. 107518, 2021. Elsevier Ltd. Disponível em: https://doi.org/10.1016/j.ecolind.2021.107518.

YAN, G.; LIU, Y.; CHEN, X. Evaluating satellite-based precipitation products in monitoring drought events in southwest China. **International Journal of Remote Sensing**, v. 39, n. 10, p. 3186–3214, 2018. Taylor & Francis. Disponível em: https://doi.org/10.1080/01431161.2018.1433892.

ZHANG, C.; GAO, X.; WANG, L.; CHEN, X. Modelling the role of epiphyton and water level for submerged macrophyte development with a modified submerged aquatic vegetation model in a shallow reservoir in China. **Ecological Engineering**, v. 81, p. 123–132, 2015. Disponível em: https://doi.org/10.1016/j.ecoleng.2015.04.048.

ZHANG, C.; LIU, H.; GAO, X.; STATE, H. Z. Modeling nutrients, oxygen and critical phosphorus loading in a shallow reservoir in China with a coupled water quality - Macrophytes model. **Ecological Indicators**, v. 66, p. 212–219, 2016. Disponível em: https://doi.org/10.1016/j.ecolind.2016.01.053.

ZHAO, D.; JIANG, H.; YANG, T.; CAI, Y.; XU, D.; AN, S. Remote sensing of aquatic vegetation distribution in Taihu Lake using an improved classification tree with modified thresholds. **Journal of Environmental Management**, 95(1), 98–107, 2012. Disponível em: https://doi.org/10.1016/j.jenvman.2011.10.007.